STABiX Documentation

Release 2.0.0

Mercier D., Zambaldi C. and Bieler T.R.

December 16, 2015

Contents

1 How to cite STABiX in your papers ? 5

2 Reference paper 7

3 Contents 9

3.1 Motivation of this Work . . . 9
3.2 Getting started . . . 10
3.3 Bicrystal Definition . . . 12
3.4 Strain Transfer Across Grain Boundaries . . . 14
3.5 Experimental data . . . 22
3.6 EBSD map GUI . . . 26
3.7 Bicrystal GUI . . . 27
3.8 CPFE simulation preprocessing GUIs . . . 31
3.9 Analysis of literature data . . . 39
3.10 A Matlab toolbox to analyze grain boundary inclination from SEM images . . . 41
3.11 References . . . 45

4 References 47

5 Contact 49

6 Contributors 51

7 Acknowledgements 53

8 Keywords 55

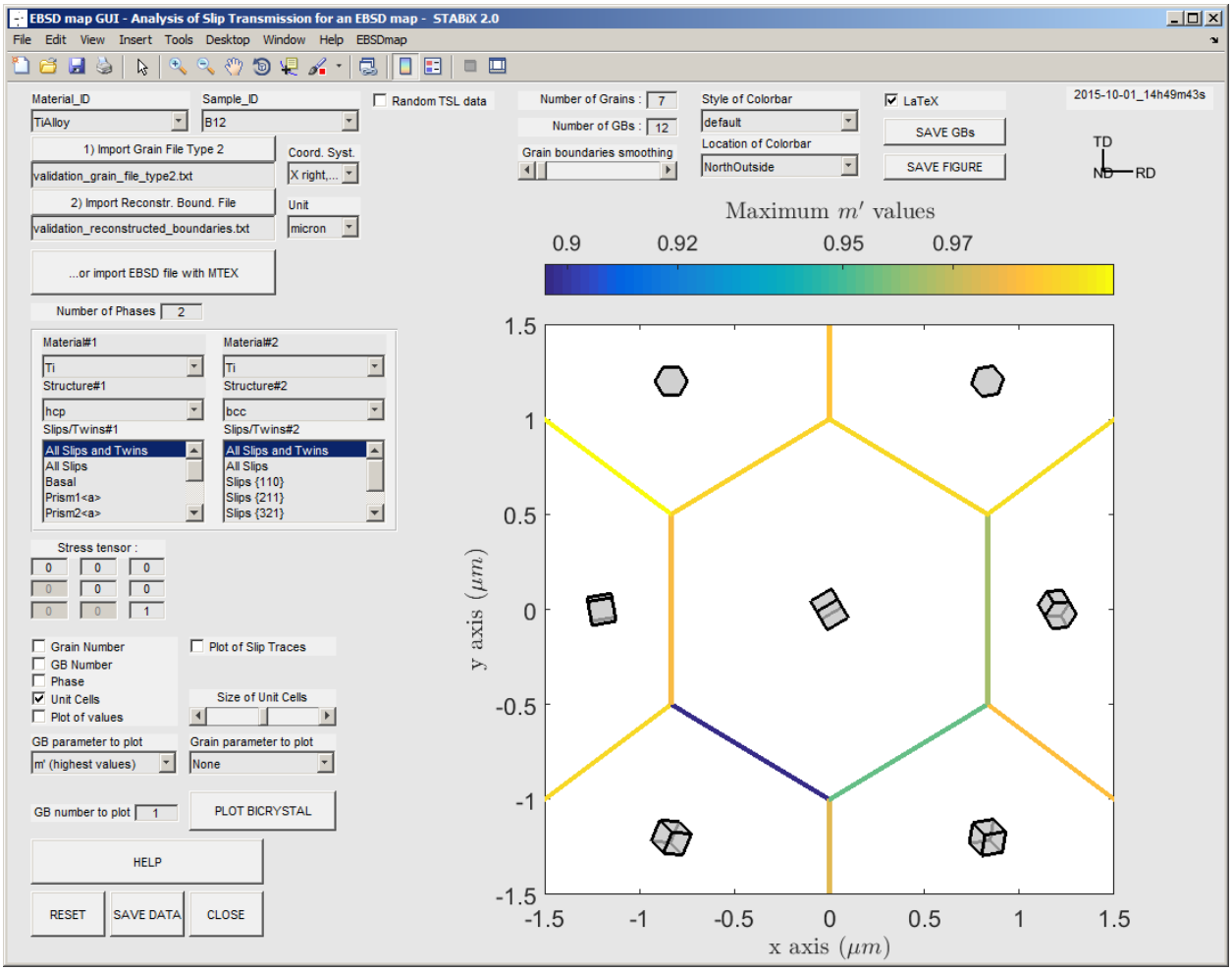

Figure 1: *Slip transmission analysis for an EBSD map of near alpha phase Ti alloy.*

The Matlab toolbox STABiX provides a unique and simple way to analyse slip transmission in a bicrystal. Graphical User Interfaces (GUIs) are implemented in order to import EBSD results, and to represent and quantify grain boundary slip resistance. Key parameters, such as the number of phases, crystal structure (fcc, bcc, or hcp), and slip families for calculations, are set by the user. With this information, grain boundaries are plotted and color coded according to the m' factor [1] that quantifies the geometrical compatibility of the slip planes normals and Burgers vectors of incoming and outgoing slip systems. Other potential functions that could assess the potential to develop damage are implemented (e.g. residual Burgers vector [2] and [3], N factor [4], resolved shear stress [5], misorientation...).

Furthermore, the toolbox provides the possibility to plot and analyze the case of a bicrystal, and to model spheroconical indentation performed in a single crystal or close to grain boundaries (i.e. quasi bicrystal deformation). All of the data linked to the bicrystal indentation (indenter properties, indentation settings, grain boundary inclination, etc.) are collected through the GUI. A python™ file can be then exported in order to carry out a fully automatic 3D crystal plasticity finite element simulations of the indentation process using one of the constitutive models available

[1] J. Luster and M.A. Morris, "Compatibility of deformation in two-phase Ti-Al alloys: Dependence on microstructure and orientation relationships.", Metal. and Mat. Trans. A (1995), 26(7), pp. 1745-1756.

[2] M.J. Marcinkowski and W.F. Tseng, "Dislocation behavior at tilt boundaries of infinite extent.", Metal. Trans. (1970), 1(12), pp. 3397-3401.

[3] W. Bollmann, "Crystal Defects and Crystalline Interfaces", Springer-Verlag (1970).

[4] J.D. Livingston and B. Chalmers, "Multiple slip in bicrystal deformation.", Acta Metallurgica (1957), 5(6), pp. 322-327.

[5] T.R. Bieler et al., "The role of heterogeneous deformation on damage nucleation at grain boundaries in single phase metals.", Int. J. of Plast. (2009), 25(9), pp. 1655–1683.

in DAMASK [6] and [7]. The plasticity of single crystals is quantified by a combination of crystal lattice orientation mapping, instrumented sphero-conical indentation, and measurement of the resulting surface topography [8] and [9]. In this way the stress and strain fields close to the grain boundary can be rapidly assessed. Activation and transmission of slip are interpreted based on these simulations and the mechanical resistance of grain boundaries can be quantified.

First of all, download the source code of the Matlab toolbox.

Source code is hosted at Github.

Download source code as a .zip file.

Find here the reference paper for this toolbox.

Download the documentation as a pdf file.

[6] F. Roters et al., "Overview of constitutive laws, kinematics, homogenization and multiscale methods in crystal plasticity finite-element modeling: Theory, experiments, applications.", Acta Materialia (2010), 58(4), pp. 1152-1211.

[7] DAMASK — the Düsseldorf Advanced Material Simulation Kit.

[8] C. Zambaldi et al., "Orientation informed nanoindentation of α-titanium: Indentation pileup in hexagonal metals deforming by prismatic slip", J. Mater. Res. (2012), 27(01), pp. 356-367.

[9] C. Zambaldi, "Anisotropic indentation pile-up in single crystals".

CHAPTER 1

How to cite STABiX in your papers ?

CHAPTER 2

Reference paper

"A Matlab toolbox to analyze slip transfer through grain boundaries" D. Mercier, C. Zambaldi, T. R. Bieler, 17th International Conference on Textures of Materials (ICOTOM17), at Dresden, Germany (2014). IOP Conference Series: Materials Science and Engineering Volume 82 conference 1. http://dx.doi.org/10.1088/1757-899X/82/1/012090

"Spherical indentation and crystal plasticity modeling near grain boundaries in alpha-Ti." D. Mercier, C. Zambaldi, P. Eisenlohr, Y. Su, M. A. Crimp, T. R. Bieler, Poster presented at "Indentation 2014" Conference in Strasbourg (France) (December 2014). http://dx.doi.org/10.13140/RG.2.1.3044.8486

CHAPTER 3

Contents

3.1 Motivation of this Work

The micromechanical behavior of grain boundaries is one of the key components in the understanding of heterogeneous deformation of metals [1]. To investigate the nature of the strengthening effect of grain boundaries, slip transmission across interfaces has been investigated through bicrystal deformation experiments during the sixty past decades [2], [3], [4], [5], [6], [7], [8], [9], [10], [11], [12], [13], [14] and [15]. Originally, interactions between dislocations and grain boundaries have been observed in the transmission electron microscope (TEM) after strain test or in situ [4], [5] and [15]. Some authors observed as well slip transmission during indentation tests performed close to grain boundaries [16], [17], [18], [19] and [20].

To better understand the role played by the grain boundaries, we developed a Matlab toolbox with Graphical User Interfaces (GUI), to analyze and to quantify the micromechanics of grain boundaries. This toolbox aims to link experimental results to crystal plasticity finite element (CPFE) simulations [21].

[1] T.R. Bieler et al., "Grain boundaries and interfaces in slip transfer.", Current Opinion in Solid State and Materials Science (2014), 18(4), pp. 212-226.

[2] K.T. Aust et al., "Solute induced hardening near grain boundaries in zone refined metals.", Acta Metallurgica (1968), 16(3), pp. 291-302.

[3] J.D. Livingston and B. Chalmers, "Multiple slip in bicrystal deformation.", Acta Metallurgica (1957), 5(6), pp. 322-327.

[4] Z. Shen et al., "Dislocation pile-up and grain boundary interactions in 304 stainless steel.", Scripta Metallurgica (1986), 20(6), pp. 921–926.

[5] Z. Shen et al., "Dislocation and grain boundary interactions in metals.", Acta Metallurgica (1988), 36(12), pp. 3231–3242.

[6] J. Luster and M.A. Morris, "Compatibility of deformation in two-phase Ti-Al alloys: Dependence on microstructure and orientation relationships.", Metal. and Mat. Trans. A (1995), 26(7), pp. 1745-1756.

[7] M.J. Marcinkowski and W.F. Tseng, "Dislocation behavior at tilt boundaries of infinite extent.", Metal. Trans. (1970), 1(12), pp. 3397-3401.

[8] W. Bollmann, "Crystal Defects and Crystalline Interfaces", Springer-Verlag (1970)

[9] L.C. Lim and R. Raj, "Continuity of slip screw and mixed crystal dislocations across bicrystals of nickel at 573K.", Acta Metallurgica (1985), 33, pp. 1577.

[10] T.C. Lee et al., "Prediction of slip transfer mechanisms across grain boundaries.", Scripta Metallurgica, (1989), 23(5), pp. 799–803.

[11] T.C. Lee et al., "An In Situ transmission electron microscope deformation study of the slip transfer mechanisms in metals", Metallurgical Transactions A (1990), 21(9), pp. 2437-2447.

[12] W.A.T. Clark et al., "On the criteria for slip transmission across interfaces in polycrystals.", Scripta Metallurgica et Materialia (1992), 26(2), pp. 203–206.

[13] W.Z. Abuzaid et al., "Slip transfer and plastic strain accumulation across grain boundaries in Hastelloy X.", J. of the Mech. and Phys. of Sol. (2012), 60(6) ,pp. 1201–1220.

[14] J.R. Seal et al., "Analysis of slip transfer and deformation behavior across the α/β interface in Ti–5Al–2.5Sn (wt.%) with an equiaxed microstructure.", Mater. Sc. and Eng.: A (2012), 552, pp. 61-68.

[15] J. Kacher et al., "Dislocation interactions with grain boundaries.", Current Opinion in Solid State and Materials Science (2014), in press.

[16] P.C. Wo and A.H.W. Ngan, "Investigation of slip transmission behavior across grain boundaries in polycrystalline Ni3Al using nanoindentation.", J. Mater. Res. (2004), 19(1), pp. 189-201.

[17] W.A. Soer et al. ,"Incipient plasticity during nanoindentation at grain boundaries in body-centered cubic metals.", Acta Materialia (2005), 53, pp. 4665–4676.

[18] T.B. Britton et al., "Nanoindentation study of slip transfer phenomenon at grain boundaries.", J. Mater. Res., 2009, 24(3), pp. 607-615.

[19] S. Patthak et al., "Studying grain boundary regions in polycrystalline materials using spherical nano-indentation and orientation imaging microscopy.", J. Mater. Sci. (2012), 47, pp. 815–823.

[20] S.K. Lawrence et al., "Grain Boundary Contributions to Hydrogen-Affected Plasticity in Ni-201.", The Journal of The Minerals, Metals & Materials Society (2014), 66(8), pp. 1383-1389.

[21] DAMASK — the Düsseldorf Advanced Material Simulation Kit

3.1.1 Strategy

Comparison of topographies of indentations at grain boundaries to simulated indentations as predicted by 3D CPFE modelling.

The goals of this research are:

1 - Carry out indentation within the interiors of large grains of alpha-titanium to effectively collect single crystal data coupled with extensive (three-dimensional) characterization of the resulting plastic defect fields surrounding the indents [22]. By correlating with models of the indentation, a precise constitutive description of the anisotropic plasticity of single-crystalline titanium shall be developed [23] and [23].

2 - Extension of this methodology to indentations close to grain boundaries, i.e. quasi bi-crystal deformation.

3 - Comparison of the measured characteristics of indentations at grain boundaries to simulated indentations as predicted by a constitutive model calibrated using the single crystal indentations.

4 - Based on this qualitative understanding, a grain boundary transmissivity description will be developed validated against the collected indent characteristics.

3.2 Getting started

3.2.1 Source Code

First of all, download the source code of the Matlab toolbox.

Source code is hosted at Github.

Download source code as a .zip file.

3.2.2 READ ME

To have more details about the use of the toolbox, please have a look to :

```
README.txt
```

3.2.3 Path management

Run the following Matlab script and answer 'y' or 'yes' to add path to the Matlab search paths :

```
path_management.m
```

The Matlab function used to set the Matlab search paths is : path_management.m

[22] C. Zambaldi et al., "Orientation informed nanoindentation of α-titanium: Indentation pileup in hexagonal metals deforming by prismatic slip", J. Mater. Res. (2012), 27(01), pp. 356-367.

[23] F. Roters et al., "Overview of constitutive laws, kinematics, homogenization and multiscale methods in crystal plasticity finite-element modeling: Theory, experiments, applications.", Acta Materialia (2010), 58(4), pp. 1152-1211.

3.2.4 The GUIs

Run one of these Graphical User Interfaces (GUIs) to play with the toolbox.

Matlab function	Features	YAML config. file
demo	Start and run other GUIs.	
EBSD map GUI	Analysis of slip transmission across GBs for an EBSD map.	config_gui_EBSDmap_defaults.yaml
Bicrystal GUI	Analysis of slip transfer in a bicrystal.	
preCPFE_SX	Preprocess of CPFE models for indentation or scratch in a SX.	config_CPFEM_defaults.yaml
preCPFE_BX	Preprocess of CPFE models for indentation or scratch in a BX.	config_CPFEM_defaults.yaml
GBinc	Calculation of grain boundaries inclination.	

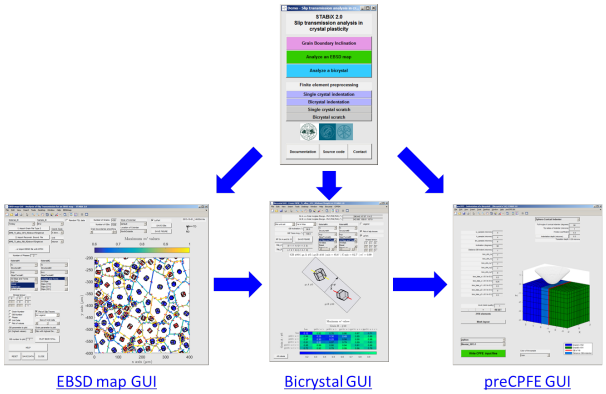

Figure 3.1: *The different GUIs of the STABiX toolbox.*

Note: 'SX' is used for single crystal and 'BX' for bicrystal.

3.2.5 The YAML configuration files

"YAML is a human friendly data serialization standard for all programming languages."

Default YAML configuration files, stored in the folder yaml_config_files, are loaded automatically to set the GUIs :

- config.yaml
- config_CPFEM_defaults.yaml
- config_CPFEM_material_defaults.yaml
- config_CPFEM_materialA_defaults.yaml
- config_CPFEM_materialB_defaults.yaml
- config_gui_EBSDmap_defaults.yaml
- config_gui_BX_defaults.yaml
- config_gui_SX_defaults.yaml
- config_mesh_BX_defaults.yaml
- config_mesh_SX_defaults.yaml

You have to set your own YAML configuration files, by following instructions given in this README.

Warning: If you create your own YAML configuration files after running STABiX, you have to run again the path_management.m Matlab function.

Visit the YAML website for more informations.

Visit the YAML code for Matlab.

3.2.6 MTEX toolbox

For some options and functions implemented in the STABiX toolbox, you have to download and install the MTEX Toolbox.

3.2.7 OpenGL

If the OpenGL rendering is not satisfying, you can modify the corresponding option in the config.yaml file.

Visit the Matlab page about OpenGL rendering.

3.3 Bicrystal Definition

3.3.1 Crystallographic properties of a bicrystal

A bicrystal is formed by two adjacent crystals separated by a grain boundary.

Five macroscopic degrees of freedom are required to characterize a grain boundary [24], [25], [26] and [27] :

- 3 for the rotation between the two crystals;
- 2 for the orientation of the grain boundary plane defined by its normal n.

The rotation between the two crystals is defined by the rotation angle ω and the rotation axis common to both crystals $[uvw]$.

Using orientation matrix of both crystals obtained by EBSD measurements, the misorientation or disorientation matrix (Δg) or (Δg_{d}) is calculated [28] and [29] :

$$\Delta g = g_{\mathrm{B}} g_{\mathrm{A}}^{-1} = g_{\mathrm{A}} g_{\mathrm{B}}^{-1} \tag{3.1}$$

$$\Delta g_{\mathrm{d}} = (g_{\mathrm{B}} * CS)(CS^{-1} * g_{\mathrm{A}}^{-1}) = (g_{\mathrm{A}} * CS)(CS^{-1} * g_{\mathrm{B}}^{-1}) \tag{3.2}$$

Disorientation describes the misorientation with the smallest possible rotation angle and CS denotes one of the symmetry operators for the material [30].

The Matlab function used to set the symmetry operators is : sym_operators.m

The orientation matrix g of a crystal is calculated from the Euler angles (ϕ_1, Φ, ϕ_2) using the following equation :

[28] V. Randle and O. Engler, "Introduction to Texture Analysis : Macrotexture, Microtexture and Orientation Mapping.", CRC Press (2000).
[29] A. Morawiec, "Orientations and Rotations: Computations in Crystallographic Textures.", Springer, 2004.
[30] U.F. Kocks et al., "Texture and Anisotropy: Preferred Orientations in Polycrystals and Their Effect on Materials Properties." Cambridge University Press (2000).

$$g = \begin{pmatrix} \cos(\phi_1)\cos(\phi_2) - \sin(\phi_1)\sin(\phi_2)\cos(\Phi) & \sin(\phi_1)\cos(\phi_2) + \cos(\phi_1)\sin(\phi_2)\cos(\Phi) & \sin(\phi_2)\sin(\Phi) \\ -\cos(\phi_1)\sin(\phi_2) - \sin(\phi_1)\cos(\phi_2)\cos(\Phi) & -\sin(\phi_1)\sin(\phi_2) + \cos(\phi_1)\cos(\phi_2)\cos(\Phi) & \cos(\phi_2)\sin(\Phi) \\ \sin(\phi_1)\sin(\Phi) & -\cos(\phi_1)\sin(\Phi) & \cos(\Phi) \end{pmatrix} \tag{3.3}$$

The orientation of a crystal (Euler angles) can be determined via electron backscatter diffraction (EBSD) measurement or via transmission electron microscopy (TEM).

The Matlab function used to generate random Euler angles is : randBunges.m

The Matlab function used to calculate the orientation matrix from Euler angles is : eulers2g.m

The Matlab function used to calculate Euler angles from the orientation matrix is : g2eulers.m

Then, from this misorientation matrix (Δg), the rotation angle (ω) and the rotation axis $[u, v, w]$ can be obtained by the following equations :

$$\omega = \cos^{-1}((tr(\Delta g) - 1)/2) \tag{3.4}$$

$$\begin{aligned} u &= \Delta g_{23} - \Delta g_{32} \\ v &= \Delta g_{31} - \Delta g_{13} \\ w &= \Delta g_{12} - \Delta g_{21} \end{aligned} \tag{3.5}$$

The Matlab function used to calculate the misorientation angle is : misorientation.m

The grain boundary plane normal n can be determined knowing the grain boundary trace angle α and the grain boundary inclination β.

The grain boundary trace angle is obtained through the EBSD measurements (grain boundary endpoints coordinates) and the grain boundary inclination can be assessed by a serial polishing (chemical-mechanical polishing or FIB sectioning), either parallel or perpendicular to the surface of the sample (see Figure 3.3).

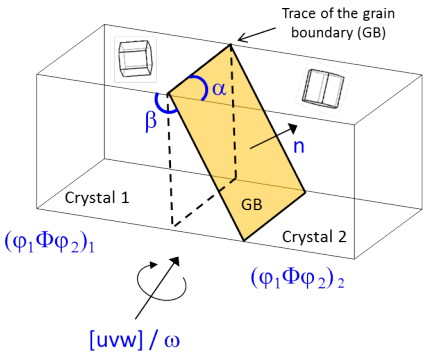

Figure 3.2: *Schematic of a bicrystal.*

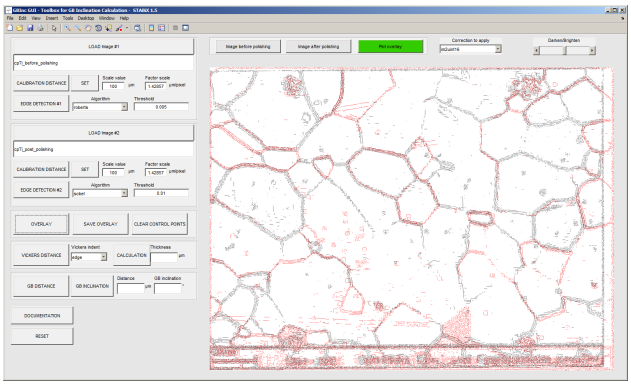

Figure 3.3: *Screenshot of the Matlab GUI used to calculate grain boundary inclination.*

3.4 Strain Transfer Across Grain Boundaries

The strain transfer across grain boundaries can be defined by the four following mechanisms (see Figure 3.4) [31], [32], [33] and [34] :

1. direct transmission with slip systems having the same Burgers vector, and the grain boundary is transparent to dislocations (no strengthening effect) (Figure 3.4-a);
2. direct transmission, but slip systems have different Burgers vector (leaving a residual boundary dislocations) (Figure 3.4-b);
3. indirect transmission, and slip systems have different Burgers vector (leaving a residual boundary dislocations) (Figure 3.4-c);
4. no transmission and the grain boundary acts as an impenetrable boundary, which implies stress accumulations, localized rotations, pile-up of dislocations... (Figure 3.4-d).

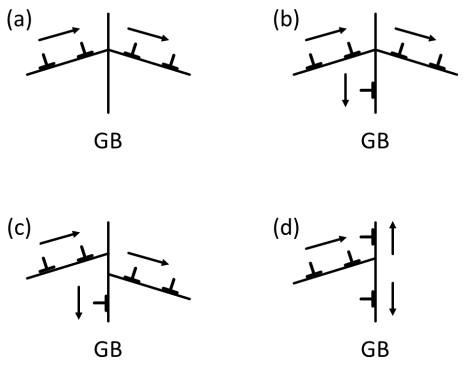

Figure 3.4: *Possible strain transfer across grain boundaries (GB) from Sutton and Balluffi.*

Several authors proposed slip transfer parameters from modellings or experiments for the last 60 years. A non-exhaustive list of those criteria is given in the next part of this work, including geometrical parameter, stress and

[31] L.C. Lim and R. Raj, "Continuity of slip screw and mixed crystal dislocations across bicrystals of nickel at 573K.", Acta Metallurgica (1985), 33, pp. 1577.
[32] A.P. Sutton and R.W. Balluffi, "Interfaces in Crystalline Materials.", OUP Oxford (1995).
[33] S. Zaefferer et al., "On the influence of the grain boundary misorientation on the plastic deformation of aluminum bicrystals.", Acta Materialia (2003), 51(16), pp. 4719-4735.
[34] L. Priester, "Grain Boundaries: From Theory to Engineering.", Springer Series in Materials Science (2013).

energetic functions, and recent combinations of the previous parameters.

3.4.1 Geometrical Criteria

Based on numerous investigations of dislocation-grain boundary interactions, quantitative geometrical expressions describing the slip transmission mechanisms have been developed. A non-exhaustive list of geometrical criteria is detailed subsequently. The geometry of the slip transfer event is most of the time described by the scheme given Figure 3.5. κ is the angle between slip directions, θ is the angle between the two slip plane intersections with the grain boundary, ψ is the angle between slip plane normal directions, γ is the angle between the direction of incoming slip and the plane normal of outgoing slip, and δ is between the direction of outgoing slip and the plane normal of incoming slip. n, d and l are respectively the slip plane normals, slip directions and the lines of intersection of the slip plane and the grain boundary. $\vec{b}$ is the Burgers vector of the slip plane and $\vec{b}_r$ is the residual Burgers vector of the residual dislocation at the grain boundary. The subscripts in and out refer to the incoming and outgoing slip systems, respectively.

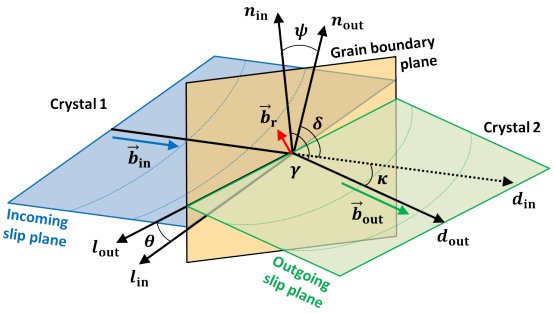

Figure 3.5: *Geometrical description of the slip transfer.*

- N **factor from Livingston and Chalmers in 1957** [35]

$$N = (\vec{n}_{in} \cdot \vec{n}_{out})(\vec{d}_{in} \cdot \vec{d}_{out}) + (\vec{n}_{in} \cdot \vec{d}_{out})(\vec{n}_{out} \cdot \vec{d}_{in}) \tag{3.6}$$

$$N = \cos(\psi) \cdot \cos(\kappa) + \cos(\gamma) \cdot \cos(\delta) \tag{3.7}$$

Many authors referred to this criterion to analyze slip transmission [36], [37], [38], [39], [40], [41], [42], [43], [44] and [45]. Pond et al. proposed to compute this geometric criteria for hexagonal metals using Frank's method [46].

[35] J.D. Livingston and B. Chalmers, "Multiple slip in bicrystal deformation.", Acta Metallurgica (1957), 5(6), pp. 322-327.
[36] J.J. Hauser and B. Chamlers, "The plastic deformation of bicrystals of f.c.c. metals.", Acta Metallurgica (1961), 9(9), pp. 802-818.
[37] K.G. Davis et al., "Slip band continuity across grain boundaries in aluminum.", Acta Metallurgica (1966), 14, pp. 1677-1684.
[38] R.E. Hook and J.P. Hirth, "The deformation behavior of isoaxial bicrystals of Fe-3%Si.", Acta Metallurgica (1967), 15(3), pp. 535-551.
[39] R.E. Hook and J.P. Hirth, "The deformation behavior of non-isoaxial bicrystals of Fe-3% Si.", Acta Metallurgica(1967), 15(7), pp. 1099-1110.
[40] Z. Shen et al., "Dislocation pile-up and grain boundary interactions in 304 stainless steel.", Scripta Metallurgica (1986), 20(6), pp. 921–926.
[41] Z. Shen et al., "Dislocation and grain boundary interactions in metals.", Acta Metallurgica (1988), 36(12), pp. 3231–3242.
[42] T.C. Lee et al., "TEM in situ deformation study of the interaction of lattice dislocations with grain boundaries in metals.", Philosophical Magazine A (1990), 62(1), pp. 131-153.
[43] T.C. Lee et al., "An In Situ transmission electron microscope deformation study of the slip transfer mechanisms in metals", Metallurgical Transactions A (1990), 21(9), pp. 2437-2447.
[44] W.A.T. Clark et al., "On the criteria for slip transmission across interfaces in polycrystals.", Scripta Metallurgica et Materialia (1992), 26(2), pp. 203–206.
[45] M. Ueda et al., "Effect of grain boundary on martensite transformation behaviour in Fe–32 at.%Ni bicrystals.", Science and Technology of Advanced Materials (2002), 3(2), pp. 171.
[46] R.C. Pond et al., "On the crystallography of slip transmission in hexagonal metals.", Scripta Metallurgica (1986), 20, pp. 1291-1295.

The Matlab function used to calculate the N factor is : N_factor.m

- LRB **factor from Shen et al. in 1986** [70] and [71]

$$LRB = (\vec{l}_{\text{in}} \cdot \vec{l}_{\text{out}})(\vec{d}_{\text{in}} \cdot \vec{d}_{\text{out}}) \tag{3.8}$$

$$LRB = \cos(\theta) \cdot \cos(\kappa) \tag{3.9}$$

The original notation of this LRB factor is M, but unfortunately this notation is often used for the Taylor factor [47]. Pond et al. proposed to compute this geometric criteria for hexagonal metals using Frank's method [62]. Recently, Spearot and Sangid have plotted this parameter as a function of the misorientation of the bicrystal using atomistic simulations [48].

[49], [47], [48], [17], [50], [51], [52], [53], [54] and [55] mentioned in their respective studies this geometrical parameter as a condition for slip transmission.

The inclination of the grain boundary (β) is required to evaluate this factor and the LRB or M factor should be maximized.

The Matlab function used to calculate the LRB factor is : LRB_parameter.m

- m' **parameter from Luster and Morris in 1995** [56]

$$m' = (\vec{n}_{\text{in}} \cdot \vec{n}_{\text{out}})(\vec{d}_{\text{in}} \cdot \vec{d}_{\text{out}}) \tag{3.10}$$

$$m' = \cos(\psi) \cdot \cos(\kappa) \tag{3.11}$$

Many authors found that this m' parameter, which takes into account the degree of coplanarity of slip systems, is promising to predict slip transmission [57], [58], [59], [60], [11], [61], [62] and [63]. Both m' and LRB can be easily assessed

[47] T.R. Bieler et al., "Grain boundaries and interfaces in slip transfer.", Current Opinion in Solid State and Materials Science, (2014), 18(4), pp. 212-226.

[48] D.E. Spearot and M.D. Sangid, "Insights on slip transmission at grain boundaries from atomistic simulations.", Current Opinion in Solid State and Materials Science (2014), in press.

[49] T.C. Lee et al., "Prediction of slip transfer mechanisms across grain boundaries.", Scripta Metallurgica, (1989), 23(5), pp. 799–803.

[50] T. Kehagias et al., "Slip transfer across low-angle grain boundaries of deformed titanium.", Interface Science (1995), 3(3), pp. 195-201.

[51] T. Kehagias et al., "Pyramidal Slip in Electron Beam Heated Deformed Titanium.", Scripta Metallurgica et Materialia (1996), 33(12), pp. 1883-1888.

[52] W.M. Ashmawi and M.A. Zikry, "Prediction of Grain-Boundary Interfacial Mechanisms in Polycrystalline Materials.", Journal of Engineering Materials and Technology (2001), 124(1), pp. 88-96.

[53] A. Gemperle et al., "Interaction of slip dislocations with grain boundaries in body-centered cubic bicrystals.", Materials Science and Engineering A (2004), 378-389, pp. 46-50.

[54] J. Gemperlova et al., "Slip transfer across grain boundaries in Fe–Si bicrystals.", Journal of Alloys and Compounds (2004), 378(1-2), pp. 97-101.

[55] J. Shi and M.A. Zikry, "Modeling of grain boundary transmission, emission, absorption and overall crystalline behavior in Σ1, Σ3, and Σ17b bicrystals.", J. Mater. Res., (2011), 26(14), pp. 1676-1687.

[56] J. Luster and M.A. Morris, "Compatibility of deformation in two-phase Ti-Al alloys: Dependence on microstructure and orientation relationships.", Metal. and Mat. Trans. A (1995), 26(7), pp. 1745-1756.

[57] M.G. Wang and A.H.W. Ngan, "Indentation strain burst phenomenon induced by grain boundaries in niobium.", Journal of Materials Research (2004), 19(08), pp. 2478-2486.

[58] P.C. Wo and A.H.W. Ngan, "Investigation of slip transmission behavior across grain boundaries in polycrystalline Ni3Al using nanoindentation.", J. Mater. Res. (2004), 19(1), pp. 189-201.

[59] T.B. Britton et al., "Nanoindentation study of slip transfer phenomenon at grain boundaries.", J. Mater. Res., (2009), 24(3), pp. 607-615.

[60] T.R. Bieler et al., "The role of heterogeneous deformation on damage nucleation at grain boundaries in single phase metals.", Int. J. of Plast. (2009), 25(9), pp. 1655–1683.

[61] Y. Guo et al., "Slip band–grain boundary interactions in commercial-purity titanium.", Acta Materialia (2014), 76, pp. 1-12.

[62] Wang F. et al., "In situ observation of collective grain-scale mechanics in Mg and Mg–rare earth alloys." Acta Materialia, (2014), 80, pp. 77–93.

[63] Y. Guo et al., "Measurements of stress fields near a grain boundary: Exploring blocked arrays of dislocations in 3D.", Acta Materialia (2015),

in computational experiments [11]. This m' factor should be maximized (1 means grain boundary is transparent and 0 means grain boundary is an impenetrable boundary).

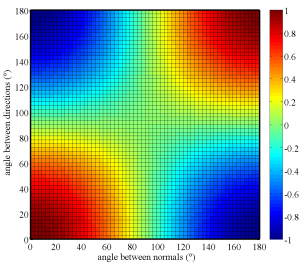

Figure 3.6: *Distribution of m' parameter in function of angles values.*

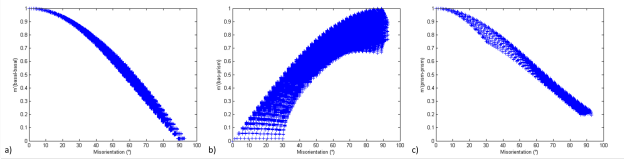

Figure 3.7: *Distributions of m' parameter calculated for a) basal vs basal slip systems, b) basal vs prismatic <a> slip systems and c) prismatic <a> vs prismatic <a> slip systems in function of misorientation angle.*

A resistance factor of the grain boundary can be described by the following equation :

$$GB_{\text{resfac}} = 1 - m' \tag{3.12}$$

This factor is equal to 0, when grain boundary is transparent to dislocations. This implies m' parameter equal to 1 (slip perfectly aligned).

The Matlab function used to calculate the m' parameter is : mprime.m

- $\vec{b}_{\text{r}}$ **the residual Burgers vector** [64], [65], [50], [66], [67], [48] **and** [17]**.**

$$\vec{b}_{\text{r}} = \vec{g}_{\text{in}} \cdot \vec{b}_{\text{in}} - \vec{g}_{\text{out}} \cdot \vec{b}_{\text{out}} \tag{3.13}$$

The magnitude of this residual Burgers vector should be minimized.

Shirokoff et al., Kehagias et al., and Kacher et al. used the residual Burgers vector as a criterion to analyse slip transmission in cp-Ti (HCP) [68], [41], [42] and [69], Lagow et al. in Mo (BCC) [70], Gemperle et al. and Gemperlova et al. in FeSi (BCC) [28] and [29], Kacher et al. in 304 stainless steel (FCC) [71], and Jacques et al. for semiconductors [72].

96, pp. 229-236.

[68] J. Shirokoff et al., "The Slip Transfer Process Through Grain Boundaries in HCP Ti.", MRS Online Proceedings Library (1993), 319, pp. 263-272.

[69] J. Kacher and I.M. Robertson, "In situ and tomographic analysis of dislocation/grain boundary interactions in α-titanium.", Philosophical Magazine (2014), 94(8), pp. 814-829.

[70] B.W. Lagow, "Observation of dislocation dynamics in the electron microscope.", Materials Science and Engineering: A, 2001, 309–310, pp. 445-450.

[71] J. Kacher and I.M. Robertson, "Quasi-four-dimensional analysis of dislocation interactions with grain boundaries in 304 stainless steel.", Acta Materialia (2012), 60(19), pp. 6657–6672.

[72] A. Jacques et al., "New results on dislocation transmission by grain boundaries in elemental semiconductors.", Le Journal de Physique Colloques (1990), 51(C1), pp. 531-536.

Patriarca et al. demonstrated for BCC material the role of the residual Burgers vector in predicting slip transmission, by analysing strain field across GBs determined by digital image correlation [73].

Misra and Gibala used the residual Burgers vector to analyze slip across a FCC/BCC interphase boundary [74].

The Matlab function used to calculate the residual Burgers vector is : residual_Burgers_vector.m

- **The misorientation or disorientation** (Δg or Δg_{d}) [75], [76] and [85]

  It has been observed during first experiments of bicrystals deformation in 1954, that the yield stress and the rate of work hardening increased with the orientation difference between the crystals [3] and [15].

  Some authors demonstrated a strong correlation between misorientation between grains in a bicrystal and the grain boundary energy through crystal plasticity finite elements modelling and molecular dynamics simulations [78], [77], [78], [79], [80] and [81]. Some authors studied the stability of grain boundaries by the calculations of energy difference vs. misorientation angle through the hexagonal c-axis/a-axis [82].

  The misorientation and disorientation equations are given in the crystallographic properties of a bicrystal.

  The Matlab function used to calculate the misorientation angle is : misorientation.m

- λ **function from Werner and Prantl in 1990** [83]

  With this function, slip transmission is expected to occur only when the angle ψ between slip plane normal directions is lower than a given critical value ($\psi_c = 15$) and the angle κ between slip directions is lower than a given critical value ($\kappa_c = 45$).

$$\lambda = \cos\left(\frac{90}{\psi_c}\arccos(\vec{n}_{\text{in}} \cdot \vec{n}_{\text{out}})\right)\cos\left(\frac{90}{\kappa_c}\arccos(\vec{d}_{\text{in}} \cdot \vec{d}_{\text{out}})\right) \tag{3.14}$$

$$\lambda = \cos\left(\frac{90\psi}{\psi_c}\right)\cos\left(\frac{90\kappa}{\kappa_c}\right) \tag{3.15}$$

  The Matlab function used to calculate the λ function is : lambda.m

  The authors proposed to plot pseudo-3D view of the λ map (see Figures 5 and 6) using the following equation [83] :

$$\lambda = \sum_{\alpha=1}^{N}\sum_{\beta=1}^{N}\cos\left(\frac{90}{\psi_c}\arccos(\vec{n}_{\text{in},\alpha} \cdot \vec{n}_{\text{out},\beta})\right)\cos\left(\frac{90}{\kappa_c}\arccos(\vec{d}_{\text{in},\alpha} \cdot \vec{d}_{\text{out},\beta})\right) \tag{3.16}$$

  With N the number of slip systems for each adjacent grains.

[73] L. Patriarca et al., "Slip transmission in bcc FeCr polycrystal.", Materials Science&Engineering (2013), A588, pp. 308–317.
[74] A. Misra and R. Gibala, "Slip Transfer and Dislocation Nucleation Processes in Multiphase Ordered Ni-Fe-Al Alloys", Metallurgical and Materials Trans. A (1999), 30A, pp. 991-1001.
[75] K.T. Aust and N.K. Chen, "Effect of orientation difference on the plastic deformation of aluminum bicrystals.", Acta Metallurgica (1954), 2, pp. 632-638.
[76] W.A.T. Clark and B. Chalmers, "Mechanical deformation of aluminium bicrystals.", Acta Metallurgica (1954), 2(1), pp. 80-86.
[77] A. Ma et al., "On the consideration of interactions between dislocations and grain boundaries in crystal plasticity finite element modeling – Theory, experiments, and simulations.", Acta Materialia (2006), 54(8), pp.2181-2194.
[78] Z. Li et al., "Strengthening mechanism in micro-polycrystals with penetrable grain boundaries by discrete dislocation dynamics simulation and Hall–Petch effect.", Computational Materials Science (2009), 46(4), pp. 1124-1134.
[79] D.V. Bachurin et al., "Dislocation–grain boundary interaction in <111> textured thin metal films.", Acta Materialia (2010), 58, pp. 5232–5241.
[80] M.D. Sangid et al., "Energy of slip transmission and nucleation at grain boundaries.", Acta Materialia (2011), 59(1), pp. 283–296.
[81] M.D. Sangid et al., "Energetics of residual dislocations associated with slip–twin and slip–GBs interactions.", Materials Science and Engineering A (2012), 542, pp. 21–30.
[82] H. Faraoun et al., "Study of stability of twist grain boundaries in hcp zinc.", Scripta Materialia (2006), 54, pp. 865–868.
[83] E. Werner and W. Prantl, "Slip transfer across grain and phase boundaries.", Acta Metallurgica et Materialia (1990), 38(3), pp. 533-537.

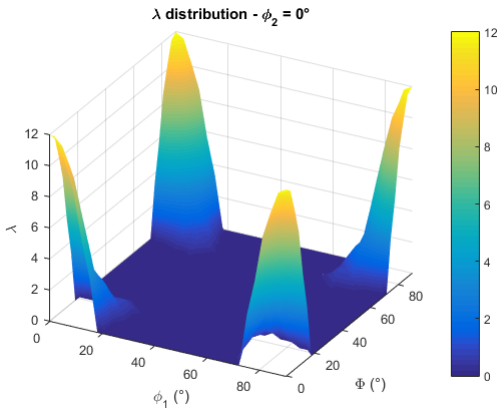

Figure 3.8: *Pseudo-3D view of the lambda map for the FCC-FCC case.*

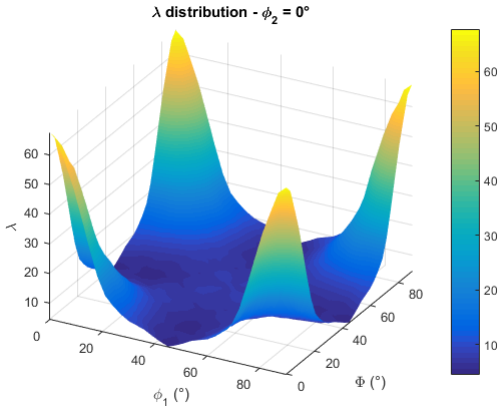

Figure 3.9: *Pseudo-3D view of the lambda map for the BCC-BCC case.*

The Matlab function used to plot pseudo-3D view of the the λ function is : lambda_plot_values.m

This function is modified by Beyerlein et al., using the angle θ between the two slip plane intersections with the grain boundary, instead of using the angle ψ between the two slip plane normal directions [84].

$$\lambda = \cos\left(\frac{90}{\theta_c}\arccos(\vec{l}_{\text{in}} \cdot \vec{l}_{\text{out}})\right)\cos\left(\frac{90}{\kappa_c}\arccos(\vec{d}_{\text{in}} \cdot \vec{d}_{\text{out}})\right) \tag{3.17}$$

$$\lambda = \cos\left(\frac{90\theta}{\theta_c}\right)\cos\left(\frac{90\kappa}{\kappa_c}\right) \tag{3.18}$$

The Matlab function used to calculate the modified λ function is : lambda_modified.m

3.4.2 Stress Criteria

- **Schmid Factor** (m) [85], [86] and [87]

  The Schmid's law can be expressed by the following equation:

$$\tau^i = \sigma : {S_0}^i \tag{3.19}$$

$${S_0}^i = \vec{d}^i \otimes \vec{n}^i \tag{3.20}$$

  σ is an arbitrary stress state and τ^i the resolved shear stress on slip system i. ${S_0}^i$ is the Schmid matrix defined by the dyadic product of the slip plane normals $\vec{n}$ and the slip directions $\vec{d}$ of the slip system i. The Schmid factor, m, is defined as the ratio of the resolved shear stress τ^i to a given uniaxial stress.

  Knowing the value of the highest Schmid factor of a given slip system for both grains in a bicrystal, Abuzaid et al. [1] proposed the following criterion :

$$m_{\text{GB}} = m_{\text{in}} + m_{\text{out}} \tag{3.21}$$

  The subscripts GB, in, and out refer to the grain boundary, and the incoming and outgoing slip systems, respectively. This GB Schmid factor (m_{GB}) factor should be maximized.

  The Matlab function used to calculate the Schmid factor is : resolved_shear_stress.m

- **Generalized Schmid Factor** (GSF) [65] and [11]

  The generalized Schmid factor, which describes the shear stress on a given slip system, can be computed from any stress tensor σ based on the Frobenius norm of the tensor.

[84] I. Beyerlein al., "Structure–Property–Functionality of Bimetal Interfaces.", The Journal of The Minerals, Metals & Materials Society (TMS) (2012), pp. 1192-1207.

[85] C.N. Reid, "Deformation Geometry for Materials Scientists.", Pergamon Press, Oxford, United Kingdom, 1973.

[86] J.R. Seal et al., "Analysis of slip transfer and deformation behavior across the α/β interface in Ti–5Al–2.5Sn (wt.%) with an equiaxed microstructure.", Mater. Sc. and Eng.: A (2012), 552, pp. 61-68.

[87] W.Z. Abuzaid et al., "Slip transfer and plastic strain accumulation across grain boundaries in Hastelloy X.", J. of the Mech. and Phys. of Sol. (2012), 60(6) ,pp. 1201–1220.

$$GSF = \vec{d} \cdot g\sigma g \cdot \vec{n} \tag{3.22}$$

$\vec{n}$ and $\vec{d}$ are respectively the slip plane normals and the slip directions of the slip system. The g is the orientation matrix for a given crystal.

The Matlab function used to calculate the generalized Schmid factor is : generalized_schmid_factor.m

- **Resolved Shear Stress** (τ) [46], [47], [48], [17], [44], [10], [88], [89] and [90]

  The resolved shear stress τ acting on the outgoing slip system from the piled-up dislocations should be maximized. This criterion considers the local stress state.

  The resolved shear stress on the grain boundary should be minimized.

  For Shi and Zikry, the ratio of the resolved shear stress to the reference shear stress of the outgoing slip system (stress ratio) should be greater than a critical value (which is approximately 1) [72].

  For Li et al. and Gao et al. the resolved shear stress acting on the incoming dislocation on the slip plane must be larger than the critical penetration stress. From the energy point of view, only when the work by the external force on the incoming dislocation is greater than the summation of the GB energy and strain energy of GB dislocation debris, it is possible that the incoming dislocation can penetrate through the GB [49] and [91].

  It is possible to assess the shear stress from the geometrical factor N (Livingston and Chamlers) :

$$\tau_{\text{in}} = \tau_{\text{out}} * N \tag{3.23}$$

  Where τ_{out} is the shear stress at the head of the accumulated dislocations in their slip plane and τ_{in} is the shear acting on the incoming slip system [52], [34] and [35].

  The Matlab function used to calculate the resolved shear stress is : resolved_shear_stress.m

3.4.3 Combination of Criteria

- **Geometrical function weighted by the accumulated shear stress or the Schmid factor** [11] :

  Bieler et al. proposed to weight slip transfer parameters by the sum of accumulated shear γ on each slip system, knowing the local stress tensor. From a crystal plasticity simulation, the accumulated shear is the total accumulated shear on each slip system for a given integration point. This leads to the following shear-informed version of a slip transfer parameter:

$$m_{\gamma}^{'} = \frac{\sum_{\alpha}\sum_{\beta} m_{\alpha\beta}^{'}\left(\gamma^{\alpha}\gamma^{\beta}\right)}{\sum_{\alpha}\sum_{\beta}\left(\gamma^{\alpha}\gamma^{\beta}\right)} \tag{3.24}$$

$$LRB_{\gamma} = \frac{\sum_{\alpha}\sum_{\beta} LRB_{\alpha\beta}^{'}\left(\gamma^{\alpha}\gamma^{\beta}\right)}{\sum_{\alpha}\sum_{\beta}\left(\gamma^{\alpha}\gamma^{\beta}\right)} \tag{3.25}$$

[88] M.P. Dewald et al., "Multiscale modelling of dislocation/grain-boundary interactions: I. Edge dislocations impinging on Σ11 (1 1 3) tilt boundary in Al.", Modelling Simul. Mater. Sci. Eng. (2007), 15(1).

[89] M.P. Dewald et al., "Multiscale modelling of dislocation/grain boundary interactions. II. Screw dislocations impinging on tilt boundaries in Al.", Phil. Mag. (2007), 87(30), pp. 1655–1683.

[90] M.P. Dewald et al., "Multiscale modeling of dislocation/grain-boundary interactions: III. 60° dislocations impinging on Σ3, Σ9 and Σ11 tilt boundaries in Al.", Modelling Simul. Mater. Sci. Eng. (2011), 19(5).

[91] Y. Gao et al., "A hierarchical dislocation-grain boundary interaction model based on 3D discrete dislocation dynamics and molecular dynamics." Science China Physics, Mechanics and Astronomy (2011), 54(4), pp. 625-632.

$$s_\gamma = \frac{\sum_\alpha \sum_\beta s'_{\alpha\beta} \left(\gamma^\alpha \gamma^\beta\right)}{\sum_\alpha \sum_\beta \left(\gamma^\alpha \gamma^\beta\right)} \tag{3.26}$$

$$s = \cos(\psi) \cdot \cos(\kappa) \cdot \cos(\theta) \tag{3.27}$$

The Matlab function used to calculate the s function is : s_factor.m

Similarly, the m' parameter can be weighted using the Schmid factor m on each slip system as a metric for the magnitude of slip transfer:

$$m'_{GSF} = \frac{\sum_\alpha \sum_\beta m'_{\alpha\beta} \left(m^\alpha m^\beta\right)}{\sum_\alpha \sum_\beta \left(m^\alpha m^\beta\right)} \tag{3.28}$$

3.4.4 Slip transmission parameters implemented in the STABiX toolbox

Slip transmission parameter	Function	Matlab function	Reference
Misorientation angle (FCC and BCC materials) (ω)	$\omega = cos^{-1}((tr(\Delta g) - 1)/2)$	misorientation.m	[78]
C-axis misorientation angle (HCP material) (ω)		c-axis misorientation.m	[78]
N factor from Livingston and Chamlers	$N = \cos(\psi)\cdot\cos(\kappa)+\cos(\gamma)\cdot\cos(\delta)$	N_factor.m	[52]
LRB factor from Shen et al.	$LRB = \cos(\theta) \cdot \cos(\kappa)$	LRB_parameter.m	[70] / [71]
m' parameter from Luster and Morris	$m' = \cos(\psi) \cdot \cos(\kappa)$	mprime.m	[53]
residual Burgers vector ($\vec{b}_\mathrm{r}$)	$\vec{b}_\mathrm{r} = g_\mathrm{in} \cdot \vec{b}_\mathrm{in} - g_\mathrm{out} \cdot \vec{b}_\mathrm{out}$	residual_Burgers_vector.m	[55]
λ function from Werner and Prantl	$\lambda = \cos(\frac{90\psi}{\psi_c}) \cos(\frac{90\kappa}{\kappa_c})$	lambda.m	[83]
Resolved Shear Stress (τ^i) / Schmid Factor	$\tau^i = \sigma : S_0{}^i$ with $S_0{}^i = d \otimes n$	resolved_shear_stress.m	[65]
Grain boundary Schmid factor	$m_\mathrm{GB} = m_\mathrm{in} + m_\mathrm{out}$	resolved_shear_stress.m	[1]
Generalized Schmid Factor (GSF)	$GSF = d \cdot g\sigma g \cdot n$	generalized_schmid_factor.m	[65]

3.4.5 Slip and twin systems implemented in the STABiX toolbox

- List of slip and twin systems for FCC phase material used in STABiX and DAMASK - FCC.
- List of slip and twin systems for BCC phase material used in STABiX and DAMASK - BCC.
- List of slip and twin systems for HCP phase material used in STABiX and DAMASK - HCP.

3.4.6 References

3.5 Experimental data

To use the STABiX toolbox, some experimental data are required :

- average grain orientations (Euler angles (ϕ_1, Φ, ϕ_2) in degrees) or intragranular misorientation (misorientation axis $[uvw]$ / angle ω);
- grains boundaries positions (optional for the bicrystal analysis);
- grains positions (optional for the bicrystal analysis);
- geometry of grain boundaries (trace angle and grain boundary inclination) (optional).

TEM experiments can provide intragranular misorientation and EBSD measurements can provide average grain orientations, grains boundaries and grains positions, and grain boundary trace angle.

Inclination of the grain boundary can be evaluated by serial polishing or focused ion beam (FIB) sectioning, either parallel or perpendicular to the surface of the sample.

3.5.1 EBSD map GUI

To plot EBSD map in the EBSD map GUI, two types of TSL-OIM files are required :

- Reconstructed Boundaries File ;
- Grain File Type 2.

TSL-OIM data preparation

Open you .osc (or your .ctf) file in the TSL-OIM Analysis Software.

Warning: Set the TSL coordinates system !

Change data properties for the detection of grain boundaries (All data –> Properties).

Clean up your dataset (Filename –> Cleanup).

Reference : OIM ANALYSIS 6.0 (user manual) and OIM ANALYSIS 7.0 (user manual) / EDAX website

Reconstructed Boundaries File

Export "Reconstructed Boundaries File" of the cleaned dataset (All data –> Export –> Reconstructed Boundaries), with the following options defined by default :

- Right hand average orientation (ϕ_1, Φ, ϕ_2) in degrees ;
- Left hand average orientation (ϕ_1, Φ, ϕ_2) in degrees ;
- Trace angle (in degrees) ;
- (x, y) coordinates of endpoints (in microns) ;
- IDs of right hand and left hand grains.

Note: Reconstructed boundary methodology is only applied to data collected on a hexagonal grid. Nevertheless, it is possible to convert a square grid into an hexagonal grid in TSL-OIM software.

Warning: It is not possible to export a "Reconstructed Boundaries File", containing "opened" grain boundaries.

Example of "Reconstructed Boundary File": MPIE_cpTi_reconstructed_boundaries_2013.txt

The Matlab function used to read "Reconstructed Boundary File" is : read_oim_reconstructed_boundaries_file.m

If some GBs segments are missing or some wrong segments are exported, play with partition properties in the TSL-OIM software in order to export a more realistic Reconstructed Boundaries file:

- decrease/increase "Grain Tolerance Angle" ;
- decrease/increase "Minimum Grain Size" ;
- decrease/increase the maximum deviation between reconstructed boundary and corresponding boundary segments.

Grain File Type 2

Export "Grain File Type 2" of the cleaned dataset (All data –> Export –> Grain File), with the following options :

- Integer identifying grain ;
- Average orientation (ϕ_1, Φ, ϕ_2) in degrees ;
- Average position (x, y) in microns ;
- An integer identifying the phase ;
- Edge or interior grain (optional) ;
- Diameter of the grain in microns (optional).

Note: Export the "Grain File Type 2" in the same location as the corresponding "Reconstructed Boundary File".

Example of "Grain Gile Type 2": MPIE_cpTi_grain_file_type2_2013.txt

The Matlab function used to read "Grain File Type 2" is : read_oim_grain_file_type2.m

Loading other type of EBSD data files...

It is possible to load other type of EBSD data files (e.g. : .ctf files), using the 'import_wizard' of the MTEX toolbox.

First, download and install the MTEX Toolbox.

Then, import your EBSD data (e.g.: .ang file) and set the coordinate systme, using the 'import_wizard' and save the EBSD dataset in the Matlab workspace as a variable named 'ebsd'.

The EBSD map is automatically plotted from the imported data. The coordinate system and the scan unit are set from the properties of the imported data.

Note: For a single phase material, the phase number is 0 or 1. For a two phases material, the phase numbers are respectively 1 and 2. For non-indexed pixels, the phase is numbered as -1.

How to generate a .ang file with TSL-OIM software ?

Export "Scan Data (.ang file)" of the cleaned dataset (Filename –> Export –> Scan Data) (optional).

Example of an .ang file.

The Matlab functions used to generate .ang file v6 and v7 are respectively:

- write_oim_ang_file_v6.m ;
- write_oim_ang_file_v7.m.

Possible errors introduced during files exportation from TSL-OIM

- **"Grain File Type 2" –> Missing integer identifying grain**
  - Solved when file is imported via the GUI.
- **"Reconstructed Boundary File" –> Inversion of left and right grains for a given grain boundary**
  - Cross product performed between GB vector and center of grains to check (if cross product < 0 : no inversion, and if cross product > 0 : inversion).
- **"Reconstructed Boundary File" –> x-axis and y-axis not corrects...**
  - y coordinates is multiplied by -1 when file is imported via the GUI.

Note: All of these issues are taken into account and corrected automatically when user is loading his data via the EBSD map GUI.

Issues with plot of EBSD maps

Sometimes, grain boundaries coordinates are too big compared to the grain size, because of the Voronoi tesselation for example. Thus, the following plot can be obtained :

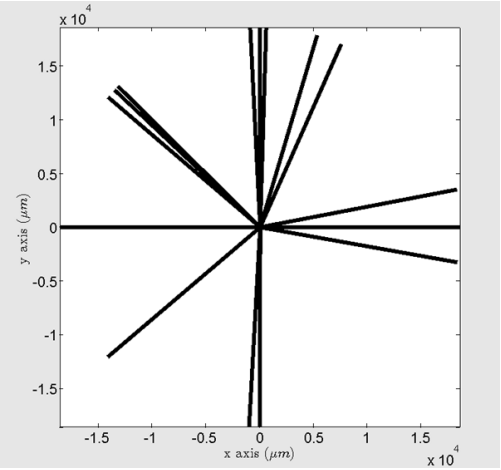

Figure 3.10: *Screenshot of the EBSD map GUI with a problem of axis limits.*

In this case, it is advised to use the 'zoom' function of Matlab to zoom in and zoom out in the center of the EBSD map, to vizualize the grains.

3.5.2 Bicrystal GUI

The YAML configuration file provides a simple way to define a bicrystal.

An example of bicrystal configuration file is given here : config_gui_BX_defaults.yaml

Copy this example file and modify it with your data. Be careful to put a space after the comma in a list (e.g. $[x, y, z]$).

Warning: Don't change fieldnames and don't round Euler angles. Euler angles are given in degrees.

Load your YAML bicrystal configuration file via the menu in the bicrystal GUI. You may have to run again the path_management.m Matlab function, if your YAML bicrystal configuration file is not found by Matlab.

Visit the YAML website for more informations.

Visit the YAML code for Matlab.

3.5.3 Convention for bicrystal EBSD/indentation experiments

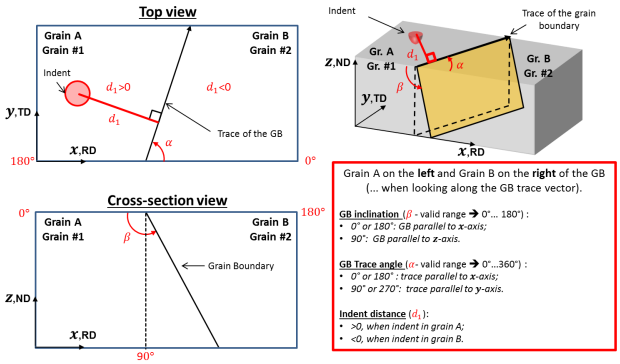

Figure 3.11: *Geometrical convention of a bicrystal.*

3.6 EBSD map GUI

This GUI allows to analyze quantitatively slip transmission across grain boundaries for an EBSD map.

The Matlab function used to run the EBSD map GUI is : A_gui_plotmap.m

This includes:

- *Loading EBSD data*
- *Smoothing GBs segments*
- *Misorientation angle*
- *m' parameter*
- *Residual Burgers vector*
- *Schmid factor and slip trace analysis*

3.6.1 Loading EBSD data

For more details about the format of the EBSD data, see also the page Experimental data.

3.6.2 Smoothing GBs segments

The smoothing algorithm allows to decrease the total number of grains boundaries in order to speed up calculations and plots.

The Matlab function used to smooth GBs is : interface_map_GB_segments_opti.m

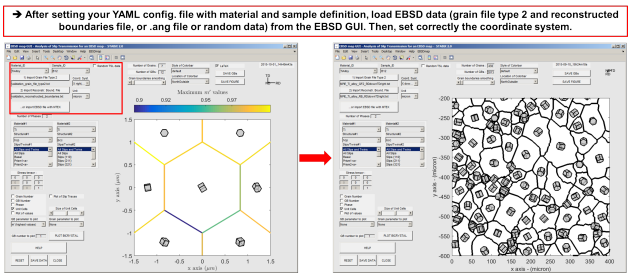
➔ After setting your YAML config. file with material and sample definition, load EBSD data (grain file type 2 and reconstructed boundaries file, or .ang file or random data) from the EBSD GUI. Then, set correctly the coordinate system.

Figure 3.12: *The different steps to load data into tge EBSD map GUI.*

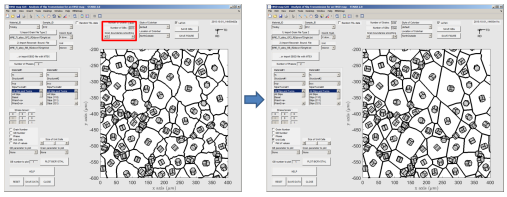

Figure 3.13: *Screenshot of the EBSD map GUI with an EBSD map of near alpha phase Ti alloy a) before smoothing and b) after smoothing.*

3.6.3 Misorientation angle

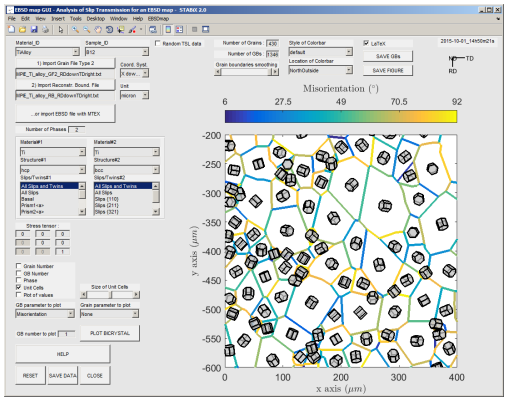

Figure 3.14: *Screenshot of the EBSD map GUI with an EBSD map of near alpha phase Ti alloy (GBs color-coded in function of the maximum misorientation angle value).*

3.6.4 m' parameter

3.6.5 Residual Burgers vector

3.6.6 Schmid factor and slip trace analysis

3.7 Bicrystal GUI

This GUI allows to analyze quantitatively slip transmission across grain boundaries for a single bicrystal.

The Matlab function used to run the Bicrystal GUI is : A_gui_plotGB_Bicrystal.m

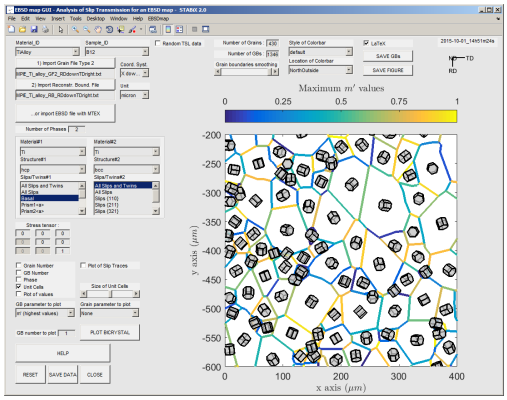

Figure 3.15: *Screenshot of the EBSD map GUI with an EBSD map of near alpha phase Ti alloy (GBs color-coded in function of the maximum m' value).*

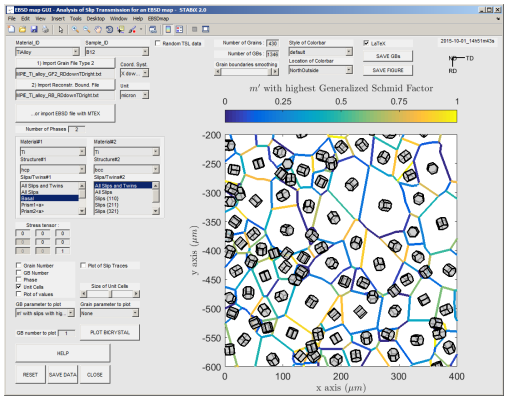

Figure 3.16: *Screenshot of the EBSD map GUI with an EBSD map of near alpha phase Ti alloy (GBs color-coded in function of the maximum m' value obtained for slips with the highest generalized Schmid factor).*

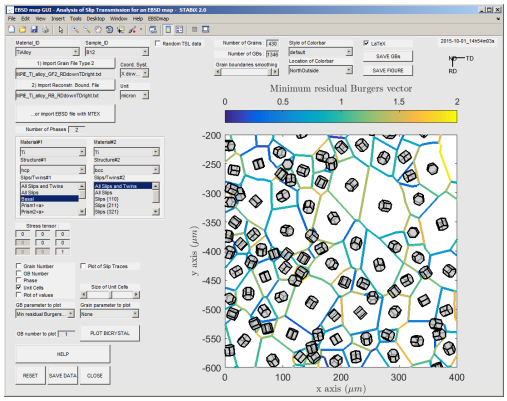

Figure 3.17: *Screenshot of the EBSD map GUI with an EBSD map of near alpha phase Ti alloy (GBs color-coded in function of the maximum residual Burgers vector value).*

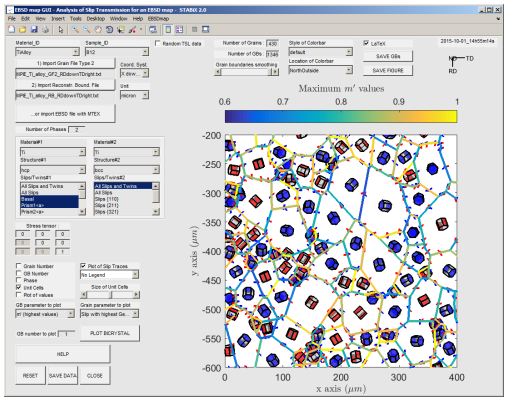

Figure 3.18: *Screenshot of the EBSD map GUI with an EBSD map of near alpha phase Ti alloy (slip plane plotted inside grain and slip traces plotted around unit cells, both in function of the maximum Schmid factor calculated with a given stress tensor).*

This includes:

- *Plotting and analyzing a bicrystal*
- *Distribution of all slip transmission parameters*

3.7.1 Loading Bicrystal data

It is possible to load bicrystal properties (material, phase, Euler angles of both grains, trace angle...) :

- from the EBSD map GUI (by giving GB number and pressing the button 'PLOT BICRYSTAL') ;
- from a YAML config. bicrystal (from the menu, by clicking on 'Bicrystal, and 'Load Bicrystal config. file').

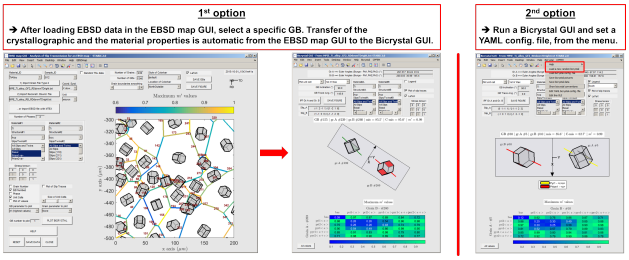
1st option
→ After loading EBSD data in the EBSD map GUI, select a specific GB. Transfer of the crystallographic and the material properties is automatic from the EBSD map GUI to the Bicrystal GUI.
2nd option
→ Run a Bicrystal GUI and set a YAML config. file, from the menu.

Figure 3.19: *The different steps to set the Bicrystal GUI.*

3.7.2 Plotting and analyzing a bicrystal

3.7.3 Distribution of all slip transmission parameters

It is possible to generate a new window, in which all values of the selected slip transmission parameter are plotted in function of selected slip families.

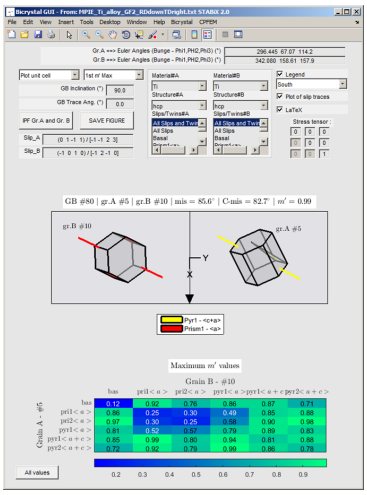

Figure 3.20: *Screenshot of the Bicrystal GUI.*

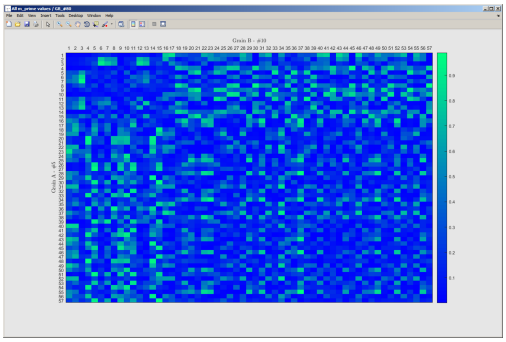

Figure 3.21: *Screenshot of the distribution of all slip transmission parameters (e.g.: m' parameter for a single phase (HCP) bicrystal).*

3.8 CPFE simulation preprocessing GUIs

The *preCPFE* GUIs can rapidly transfer the experimental data into crystal plasticity finite element (CPFE) simulation input files. The types of input files are :

- scripts to generate the finite element models in *MSC.Mentat* (2008 to 2014) (*procedure* file format) or *Abaqus* (6.12 to 6.14) (Python script) based on the experimental data and test geometry ;
- the crystallographic orientations from the experimental data sets ;
- material parameter files for the subroutines that implement the constitutive model.

A parametrized visualization of the bicrystal indentation model through the GUI allows tuning the geometry and finite element discretization and the size of the sample and the indenter.

Currently the following models can be written:

- *Single crystal (SX) indentation* (MSC.Mentat and Abaqus)
- *Bicrystal (BX) indentation* (MSC.Mentat and Abaqus)
- *Scratch test on SX and BX* (MSC.Mentat and Abaqus)

Please find here the Python package used to generate the SX and BX indentation models.

3.8.1 How to load crystallographic properties of the SX or of the BX ?

It is possible to set SX or BX properties (material, phase, Euler angles, trace angle...) :

- from the Bicrystal GUI (by giving GB's number and pressing the button 'PLOT BICRYSTAL');
- from a YAML configuration file (from the menu, by clicking on 'preCPFE-SX' or 'preCPFE-BX', and 'Load Single Crystal config. file' or 'Load Bicrystal config. file').

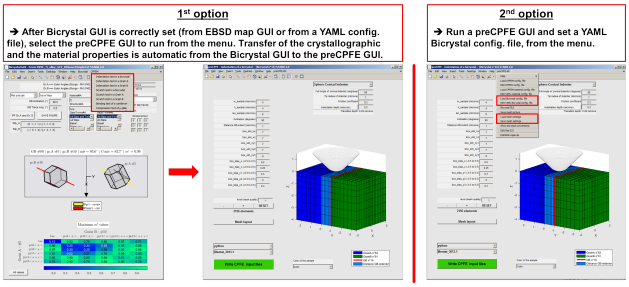
1st option
→ After Bicrystal GUI is correctly set (from EBSD map GUI or from a YAML config. file), select the preCPFE GUI to run from the menu. Transfer of the crystallographic and the material properties is automatic from the Bicrystal GUI to the preCPFE GUI.
2nd option
→ Run a preCPFE GUI and set a YAML Bicrystal config. file, from the menu.

Figure 3.22: *The different steps to set the preCPFE GUIs.*

3.8.2 Single crystal (SX) indentation

Analysis of the orientation dependent pile-up topographies that are formed during single crystal indentation provides insight into the operating deformation mechanisms. CPFE simulation of single crystal indentation has an important role in clarifying the influence of the single-slip behaviour of different slip systems on the resulting surface profiles.

The function used to run the preCPFE GUI for SX indentation is : A_preCPFE_windows_indentation_setting_SX.m

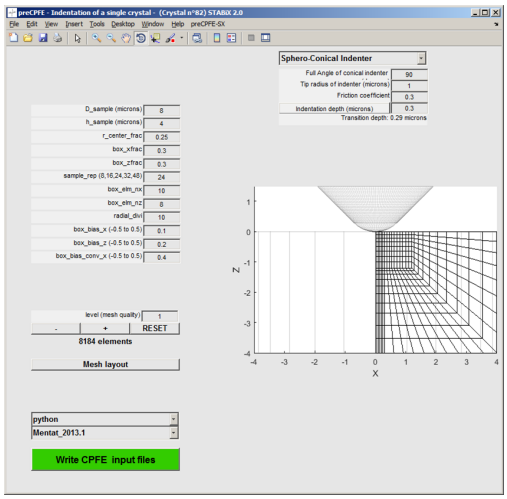

Figure 3.23: *Screenshot of the preCPFE GUI for the single crystal indentation*

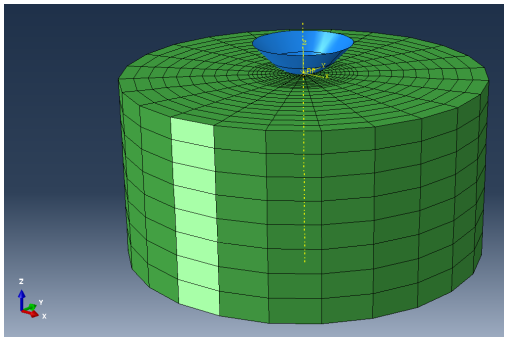

Figure 3.24: *Screenshot of the single crystal indentation model in Abaqus.*

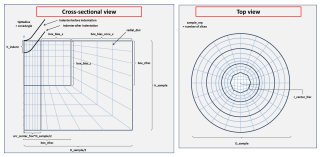

Figure 3.25: *Convention used to define the single crystal mesh.*

Convention for the single crystal mesh

3.8.3 Bicrystal (BX) indentation

CPFE simulation of indentation close to grain boundaries can provide a good approximation of the local micromechanics in this experiment. While models that take into account the micromechanical effect of the boundary are the subject of ongoing research, most geometrical and kinematic factors are taken into account by employing a local phenomenological crystal plasticity formulation in the simulations.

The function used to run the preCPFE GUI for BX indentation is : A_preCPFE_windows_indentation_setting_BX.m

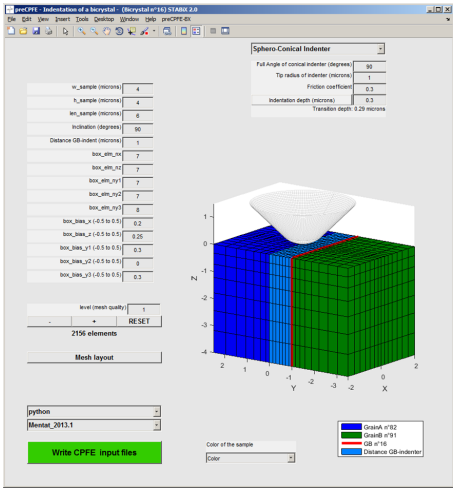

Figure 3.26: *Screenshot of the preCPFE GUI for the bicrystal indentation.*

Convention for the bicrystal mesh

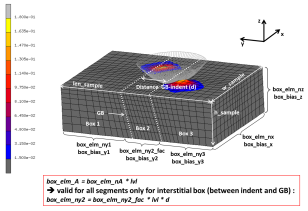
Indenter
Distance GB-indent (d)
GB
Box 1
Box 2
Box 3
box_elm_A = box_elm_nA * lvl
→ valid for all segments only for interstitial box (between indent and GB) :
box_elm_ny2 = box_elm_ny2_fac * lvl * d

Figure 3.27: *Convention used to define the bicrystal mesh.*

3.8.4 Scratch test on SX and BX

CPFE simulation of scratch test in a single crystal or close to a grain boundary is implemented into this GUI. Scratch length and scratch direction have to be set by the user.

3.8.5 Indenter's geometry

Currently the following geometries can be used for CPFE simulations :

- cono-spherical indenter ;

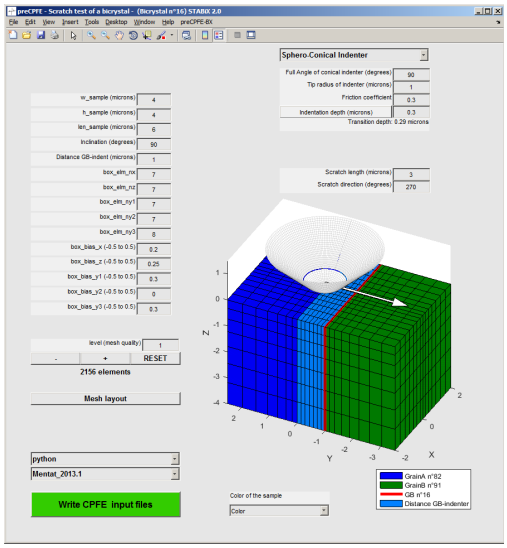

Figure 3.28: *Screenshot of the preCPFE GUI for the scratch test.*

- Berkovich indenter ;
- Vickers indenter ;
- cube corner indenter ;
- flat punch ;
- free topography (from an AFM measurement for instance).

For the Berkovich, Vickers, cube corner indenters and the free topography, the faces and vertices are saved in a structure variable from a patch object. For the cono-spherical and the flat punch, geometries are already implemented in the Python package for *MSC.Mentat* and *Abaqus*. It is possible as well to call the Matlab function surf2patch, to return the faces and vertices from a surface object.

Then the function patch2inp is used to generate an *Abaqus .inp* file, which is used when the CPFE model is created in *MSC.Mentat* or *Abaqus*.

It is possible to rotate directly into the GUIs, the Berkovich, Vickers, cube corner indenters and the free topography before the generation of the *Abaqus .inp* file.

AFM topography

The topography from an Atomic Force Microscopy (AFM) measurement has to be saved into a .txt file in the *Gwyddion ASCII* format.

The Matlab function used to load and read Gwyddion file is : read_gwyddion_ascii.m

Visit the Gwyddion website for more information.

3.8.6 Contact definition

- ***MSC.Mentat***
  - The indenter is modeled by a rigid body and the sample by a deformable body.
  - Contact is defined by a bilinear Coulomb friction model.

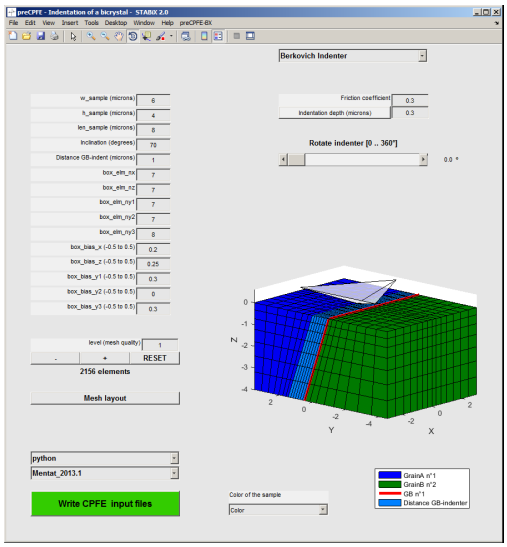

Figure 3.29: *Screenshot of the preCPFE GUI for the bicrystal indentation with Berkovich indenter.*

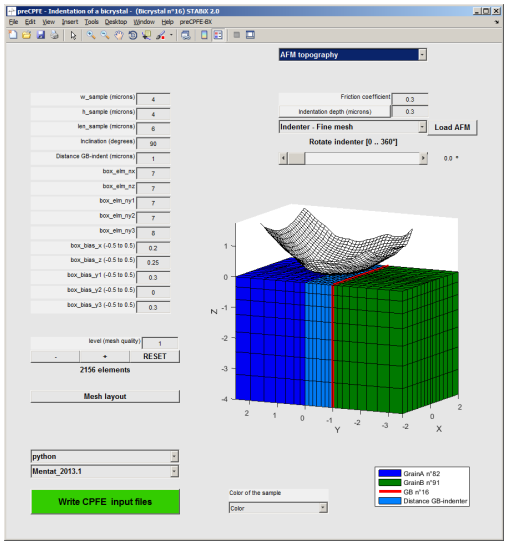

Figure 3.30: *Screenshot of the preCPFE GUI for the bicrystal indentation with loaded AFM topography of the indenter.*

- ***Abaqus***
  - The indenter is modeled by a rigid body and the sample by a deformable body.
  - The external surface of the indenter is defined as the "master" region.
  - The top surface of the (multilayer) sample is defined as the "slave" region.
  - If the coefficient friction is different from 0, the classical isotropic Coulomb friction model is used to define the contact between the indenter and the sample.
  - If the coefficient friction is set to 0, the contact is defined by a frictionless tangential behavior and a hard normal behavior.

A friction coefficient of 0.3 is set by default for every CPFE simulation. It is possible to modify this parameter, by changing its value in the *preCPFE* GUIs.

3.8.7 Mesh definition

- ***MSC.Mentat***
  - The mesh is defined by default by hexahedral eightnode elements (hex8).
- ***Abaqus***
  - The mesh is defined by default by linear hexahedral eightnode elements (C3D8).
  - It is possible to set quadratic elements (e.g.: C3D20), by changing in the python code the value of the "linear_elements" variable from 1 to 0.

Note: Note that DAMASK incorporates a limited number of different types of element geometries. For a detailed information about the characteristics of each element refer to MSC.Marc and Abaqus user's manuals.

3.8.8 Python setup

For the generation of the CPFE preprocessing scripts an installation of Python is required together with the *Numpy* package. Often one of the scientific Python distributions is the easiest way to get up and running (use a Python 2.x distribution). To make sure that STABiX can find the installed Python you will have to either put it on the system's PATH or put it's exact location in the user configuration as detailed below.

3.8.9 Adjusting the configuration settings

To write out the necessary files for finite element simulations it is likely that the user wants to adjust some settings such as the used python installation or the path where the files are written to. This can be achieved in the custom menu of the preCPFE GUis : `Edit CPFEM config file`. A user specific copy of the default configuration YAML file is created and opened in the Matlab editor. To benefit from later changes in the default settings, all configuration parameters that are not specific to the user's setup should be deleted from the user's CPFE configuration file.

3.8.10 Installing DAMASK

For instructions on how to set up the DAMASK constitutive simulation code please visit http://DAMASK.mpie.de.

3.8.11 Writing the CPFE input files

After everything is configured and the model geometry and discretization is optimized, all necessary files to run a CPFE simulation can be generated by pressing the green button. All information will be written to a newly created folder which also includes a timestamp for later reference.

3.8.12 Input files

- ***MSC.Mentat***
  - a procedure file containing the FEM model (*.proc)
  - a Python file containing parameters for FEM model (*.mat_FEM_model_parameters.py)
  - a Python file containing material configuration (*.mat_DAMASK_materialconfig.py)
  - a MAT-file (binary Matlab format file) storing Matlab workspace variables(*.mat)
  - a material configuration file (material.config)
  - an input file for specific indenter's geometry (*.inp) (optional)
- ***Abaqus***
  - a Python file containing the FEM model (*.py)
  - a Python file containing parameters for FEM model (*.mat_FEM_model_parameters.py)
  - a Python file containing material configuration (*.mat_DAMASK_materialconfig.py)
  - a MAT-file (binary Matlab format file) storing Matlab workspace variables(*.mat)
  - a material configuration file (material.config)
  - an input file for specific indenter's geometry (*.inp) (optional)

3.8.13 Using the CPFE input files

- ***MSC.Mentat 'classic interface'***
  - 'Files' ==> 'Current Directory' ==> Select the folder containing input files
  - 'Utils' ==> 'Procedures' ==> Select procedure file containing the FEM model (*.proc)
- ***MSC.Mentat 'new interface (> 2012)'***
  - 'Files' ==> 'Current Directory' ==> Select the folder containing input files
  - 'Tools' ==> 'Procedures' ==> Select procedure file containing the FEM model (*.proc)
- ***Abaqus***
  - 'File' ==> 'Set Work Directory...' ==> Select the folder containing input files
  - 'File' ==> 'Run Script' ==> Select the Python file containing the FEM model (*.py)

3.8.14 Running a job with DAMASK

- ***MSC.Mentat***
  - In the JOB RUN menu choose USER SUBROUTINE FILE and select the interface routine DAMASK_marc.f90.

Find the full documentation for the use of DAMASK with Marc here : http://damask.mpie.de/Usage/Marc.

- ***Abaqus***
  - In the Job Manager > Create... specify the User subroutine file (either DAMASK_abaqus_std.f or DAMASK_abaqus_exp.f).

Find the full documentation for the use of DAMASK with Abaqus here : http://damask.mpie.de/Usage/Abaqus.

Note:

For Abaqus, you may have to modify the extension of the subroutine :

- .f if the operating environment is Linux ;
- .for if the operating environment is Windows.

3.8.15 See also

Wang Y. et al., "Orientation dependence of nanoindentation pile-up patterns and of nanoindentation microtextures in copper single crystals.", Acta Materialia (2004).

Liu Y. et al., "Combined numerical simulation and nanoindentation for determining mechanical properties of single crystal copper at mesoscale.," Journal of the Mechanics and Physics of Solids (2005).

Zaafarani N. et al., "Three-dimensional investigation of the texture and microstructure below a nanoindent in a Cu single crystal using 3D EBSD and crystal plasticity finite element simulations.", Acta Materialia (2006).

Zambaldi C. et al., "Modeling and experiments on the indentation deformation and recrystallization of a single-crystal nickel-base superalloy.", Materials Science and Engineering A (2007).

Liu Y. et al., "Orientation effects in nanoindentation of single crystal copper.", International Journal of Plasticity (2008).

Zaafarani N. et al., "On the origin of deformation-induced rotation patterns below nanoindents.", Acta Materialia (2008).

Casals O. and Forest S., "Finite element crystal plasticity analysis of spherical indentation in bulk single crystals and coatings.", Computational Materials Science (2009).

Gerday A. F. et al., "Interests and limitations of nanoindentation for bulk multiphase material identification: Application to the β phase of Ti-5553.", Acta Materialia (2009).

Britton T.B. et al., "The effect of crystal orientation on the indentation response of commercially pure titanium: experiments and simulations.", Proc. R. Soc. A (2010).

Chang H.-J. et al., "Multiscale modelling of indentation in FCC metals: From atomic to continuum.", C. R. Physique (2010).

Zambaldi C. and Raabe D., "Crystal plasticity modelling and experiments for deriving microstructure-property relationships in γ-TiAl based alloys.", Journal of Physics (2010).

Zambaldi C., "Micromechanical modeling of γ-TiAl based alloys.", PhD Thesis (2010).

Zambaldi C. and Raabe D., "Plastic anisotropy of c-TiAl revealed by axisymmetric indentation.", Acta Materialia (2011).

Vu-Hoang S. et al., "Crystal Plasticity of Single Crystal and Film on Substrate Probed by Nano-Indentation: Simulations and Experiments.", Mater. Res. Soc. Symp. Proc. (2011).

Eidel B., "Crystal plasticity finite-element analysis versus experimental results of pyramidal indentation into (001) fcc single crystal.", Acta Materialia (2011).

Zambaldi C. et al., “Orientation informed nanoindentation of a-titanium: Indentation pileup in hexagonal metals deforming by prismatic slip.”, J. Mater. Res. (2012).

Zahedi A. et al., “Indentation in f.c.c. single crystals.”, Solid State Phenomena (2012).

Liu M. et al., “Crystal Plasticity Study of the Effect of the Initial Orientation on the Indentation Surface Profile Patterns and Micro-Textures of Aluminum Single Crystal”, Advances in Materials and Processing Technologies (2013).

Han F. et al., “Experiments and crystal plasticity finite element simulations of nanoindentation on Ti-6Al-4 V alloy.”, Materials Science & Engineering A (2014).

Choudhury S.F. et al., “Single Crystal Plasticity Finite Element Analysis of Cu6Sn5 Intermetallic.”, Metall. and Mat. Trans. A (2014).

González D. et al., “Numerical analysis of the indentation size effect using a strain gradient crystal plasticity model.”, Computational Materials Science (2014).

Esqué-de los Ojos D. et al., “Sharp indentation crystal plasticity finite element simulations: Assessment of crystallographic anisotropy effects on the mechanical response of thin fcc single crystalline films.”, Computational Materials Science (2014).

Kitahara H. et al., “Anisotropic deformation induced by spherical indentation of pure Mg single crystals.”, Acta Materialia (2014).

Kucharski S. et al., “Surface Pile-Up Patterns in Indentation Testing of Cu Single Crystals.”, Experimental Mechanics (2014).

Liu M. et al., “A crystal plasticity study of the effect of friction on the evolution of texture and mechanical behaviour in the nano-indentation of an aluminium single crystal.”, Computational Materials Science (2014).

Yao W.Z. et al., “Plastic material parameters and plastic anisotropy of tungsten single crystal: a spherical microindentation study.”, J. Mater. Sci. (2014).

Charleux L., “Abapy Documentation”.

CPFEM simulations of nanoindentation - ongoing research.

Zambaldi C. et al., “Orientation dependent deformation by slip and twinning in magnesium during single crystal indentation”, Acta Materialia (2015).

Sánchez-Martín R. et al., “High temperature deformation mechanisms in pure magnesium studied by nanoindentation”, Scripta Materialia (2015).

Mao L. et al., “Explore the anisotropic indentation pile-up patterns of single-crystal coppers by crystal plasticity finite element modelling”, Materials Letters (2015).

Mao L. et al., “Crystal plasticity FEM study of nanoindentation behaviors of Cu bicrystals and Cu–Al bicrystals”, J. Mater. Res., (2015).

Renner E. et al., “Sensitivity of the residual topography to single crystal plasticity parameters in Berkovich nanoindentation on FCC nickel”, International Journal of Plasticity, (2015).

Juran P. et al., “Investigation of indentation-, impact- and scratch-induced mechanically affected zones in a copper single crystal”, Comptes Rendus Mécanique, (2015).

Materna A. et al., “A Numerical Investigation of the Effect of Cubic Crystals Orientation on the Indentation Modulus”, Acta Physica Polonica A, (2015).

3.9 Analysis of literature data

Please, find here the Matlab functions to analyze results and to plot data from the following papers.

3.9.1 Residual Burgers vector

Kacher and Robertson (2012)

Kacher and Robertson analyzed slip transfer in 304 stainless steel (FCC structure), using in situ TEM deformation [92]. In this work, a bicrystal with a misorientation angle of 36° and misorientation axis of [-11, -22, -2] is characterized. Dislocation/grain boundary interactions are analysed and knowing the incoming system, the magnitude of residual dislocation Burgers vector is plotted in function of possible outgoing systems. Calculations are reproduced using the Matlab toolbox and obtained values are compared to Kacher's results (see Figure 3.31).

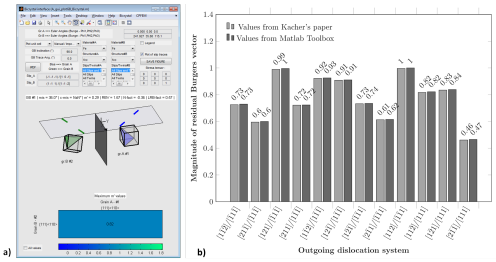

Figure 3.31: *a) Plot of a bicrystal with a misorientation angle of 36°and misorientation axis of [-11, -22, -2] from Kacher's paper. b) Magnitude of residual Burgers vector given in Kacher's paper compared to values calculated with the Matlab toolbox.*

Patriarca et al. (2013)

Patriarca et al. analysed the deformation response of a FeCr polycrystal (BCC structure) by a combination of EBSD and digital image correlation (DIC) characterizations [93]. The magnitude of residual dislocation Burgers vector is plotted for numerous grain boundaries, knowing incoming and outgoing slips. Calculations are reproduced using the Matlab toolbox and results are compared to Patriarca's results (see Figure 3.32).

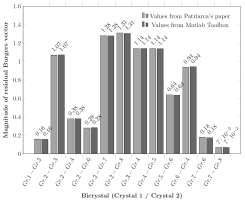
Values from Patriarca's paper
Values from Matlab Toolbox
Magnitude of residual Burgers vector
Bicrystal (Crystal 1 / Crystal 2)

Figure 3.32: *Magnitude of residual Burgers vector given in Patriarca's paper compared to values calculated with the Matlab toolbox for numerous grain boundaries.*

Kacher and Robertson (2014)

Kacher and Robertson analyzed slip transfer in alpha cp-Ti (HCP structure), using in situ TEM deformation [94]. In this work, a bicrystal with a misorientation angle of 32° and misorientation axis of [1, 5, -6, 16] is characterized. Dislocation/grain boundary interactions are analysed and knowing the incoming system, the magnitude of residual

[92] J. Kacher and I.M. Robertson, "Quasi-four-dimensional analysis of dislocation interactions with grain boundaries in 304 stainless steel.", Acta Materialia (2012), 60(19), pp. 6657–6672.

[93] L. Patriarca et al., "Slip transmission in bcc FeCr polycrystal.", Materials Science&Engineering (2013), A588, pp. 308–317.

[94] J. Kacher and I.M. Robertson, "In situ and tomographic analysis of dislocation/grain boundary interactions in α-titanium.", Philosophical Magazine (2014), 94(8), pp. 814-829.

dislocation Burgers vector is plotted in function of possible outgoing systems. Calculations are reproduced using the Matlab toolbox and obtained values are compared to Kacher's results (see Figure 3.33).

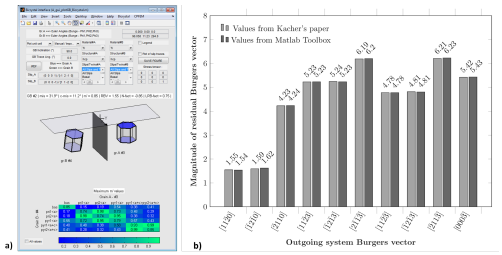

Figure 3.33: *a) Plot of a bicrystal with a misorientation angle of 32° and misorientation axis of [1, 5, -6, 16] from Kacher's paper. b) Magnitude of residual Burgers vector given in Kacher's paper compared to values calculated with the Matlab toolbox for the bicrystal #2.*

Cui et al. (2014)

Cui et al. analyzed slip transfer in proton-irradiated 13Cr15Ni stainless steel (fcc structure), using in situ TEM deformation [95]. In this work, two bicrystals with respectively a misorientation angles of 60° and 40° and a misorientation axis of [1, 1, -1] and [1, 0, 1] are characterized. Dislocation/grain boundary interactions are analysed and knowing the incoming system, the magnitude of residual dislocation Burgers vector is plotted in function of possible outgoing systems. Calculations are reproduced using the Matlab toolbox and obtained values are compared to Cui's results (see Figure 3.34).

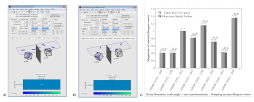

Figure 3.34: *a) Plot of a bicrystal with a misorientation angle of 60° and misorientation axis of [1, 1, -1] from Cui's paper. b) Plot of a bicrystal with a misorientation angle of 40° and misorientation axis of [1, 0, 1] from Cui's paper. c) Magnitude of residual Burgers vector given in Cui's paper compared to values calculated with the Matlab toolbox for the two bicrystals.*

3.9.2 m' factor

Guo et al. (2014)

Guo et al. analyzed slip transfer in cp-Ti (HCP structure), by tensile test combined to in situ digital image correlation (DIC) [96]. In this work, many bicrystals are characterized and slip band–grain boundary interactions are analyzed in term of stress concentration along the slip plane direction. The m' factor is used to quantify the transmissivity across the GBs and calculations are reproduced using the Matlab toolbox (see Figure 3.35).

3.10 A Matlab toolbox to analyze grain boundary inclination from SEM images

First of all, download the source code of the Matlab toolbox.

[95] B. Cui et al., "Influence of irradiation damage on slip transfer across grain boundaries.", Acta Materialia (2014), 65, pp. 150-160.
[96] Y. Guo et al., "Slip band–grain boundary interactions in commercial-purity titanium.", Acta Materialia (2014), 76, pp. 1-12.

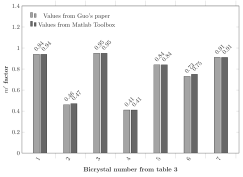

Figure 3.35: *m' factor values given in Guo's paper compared to values calculated with the Matlab toolbox for 7 different bicrystals.*

Source code is hosted at Github.

Download source code as a .zip file.

This toolbox helps to find the grain boundary inclination from two micrographs from serial polishing. At least three marks such as microindents are needed for registration of the images.

Examples of micrographs from serial polishing.

To get started with this toolbox, clone the repository, then run Matlab, and cd into the folder containing this README file. Then add the package path to the Matlab search path by typing "path_management". Finally you can start the launcher by typing demo or A_gui_gbinc at the Matlab command prompt.

3.10.1 How to use the toolbox ?

1. Run the function A_gui_gbinc.m.
2. Select your first image before serial polishing.
3. Do the calibration to get the factor scale.
4. Do the edge detection.
5. Repeat the same operation for the second image obtained after serial polishing.
6. Do the overlay :
   - If control points don't exist (it's the case for the 1st time), a window appears and it is possible to define control points.
   - Define 3 control points per images.
   - Select a point on the figure on the left, then on the figure on the right, and repeat this operation 2 times.
   - Close the window for the selection of control points (Ctrl+W).
   - Control points are saved in .mat file (in the same folder than the 1st picture loaded).
7. If the control points are not satisfying, delete them and redo the step 6 to set new control points and to get a new overlay.
8. Save the overlay in the same folder than the 1st picture loaded (as a screenshot.png) (optional).
9. Do the measurement of the distance between edges (Vickers faces) or ridges of a unique Vickers indent (see Figure 3.37).
10. Do the measurement of the distance between edges of a unique grain boundary.

11. The value of the grain boundary inclination is finally given in degrees.

- Calculation of the thickness of removed material after polishing

$$h = \frac{d}{\tan(90 - \alpha)} \tag{3.29}$$

With d the distance between edges (Vickers faces) or ridges of a unique Vickers indent (obtained before and after polishing), and α the angle between the Vickers indent and the surface of the sample (see Figure 3.37).

- Calculation of grain boundary inclination

$$GB_{inc} = \tan\left(\frac{d_{GB}}{h}\right) \tag{3.30}$$

With d_{GB} the distance between grain boundary traces (obtained before and after polishing), and h the thickness of removed material after polishing calculated

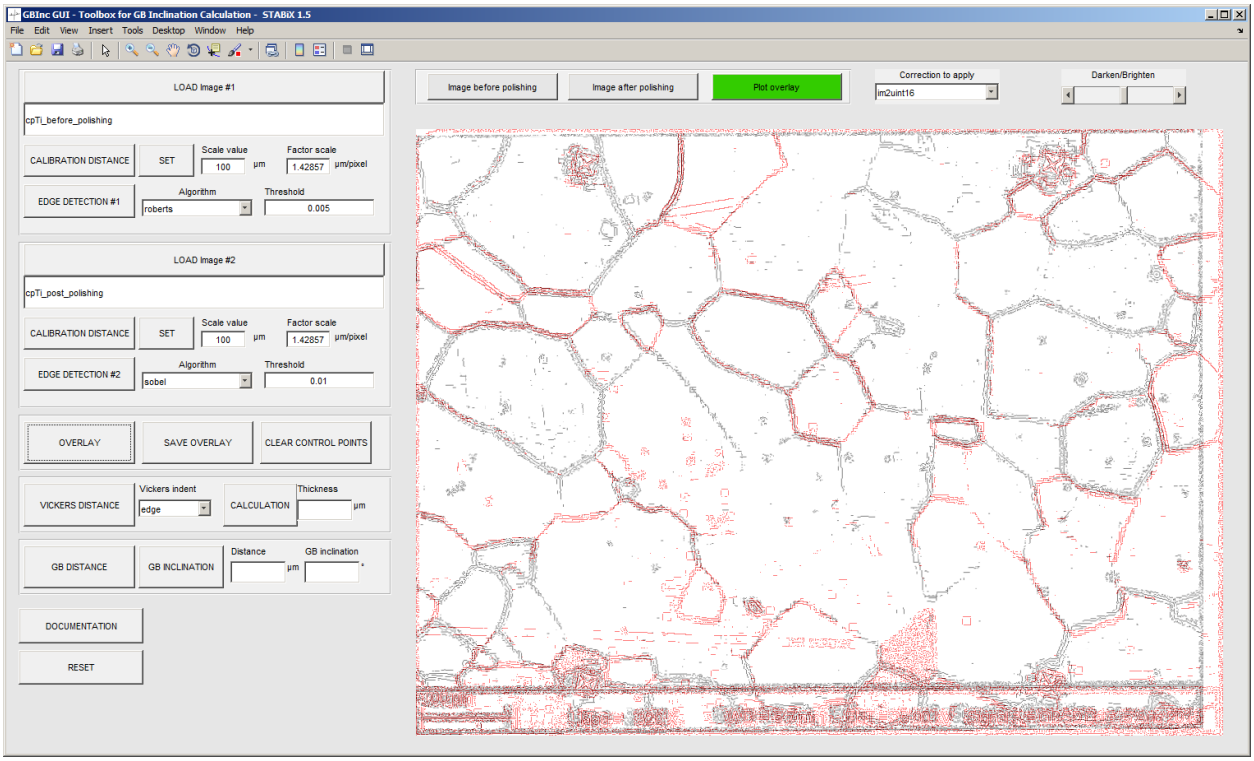

Figure 3.36: *Screenshot of the Matlab GUI used to calculate grain boundary inclination.*

Note: Images should have the same scale factor.

Note: Distances and grain boundary inclination values are obtained with the mean scale factor of the two images.

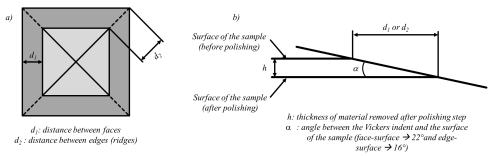
a)
b)
Surface of the sample (before polishing)
Surface of the sample (after polishing)
h
α
h: thickness of material removed after polishing step
α : angle between the Vickers indent and the surface of the sample (face-surface → 22°and edge-surface → 16°)

Figure 3.37: *Schemes of a) the top view of a Vickers indent (before and after polishing) and of b) the cross-section view.*

3.10.2 See also

V. Randle and Dingley D., "Measurement of boundary plane inclination in a scanning electron microscope.", Scripta Metall., 1989, 23, pp. 1565–1569.

V. Randle, "A methodology for grain boundary plane assessment by single-section trace analysis.", Scripta Mater., 2001, 44, pp. 2789-2794.

3.10.3 Links

- Matlab - Interactive Exploration with the Image Viewer App
- Matlab - Distance tool
- Matlab - Image conversions
- Matlab - Image filtering
- Matlab - Control Point Selection Tool
- Matlab - Spatial transformation from control point pairs
- Matlab - Edge detection

3.10.4 Authors

Written by D. Mercier [1] and C. Zambaldi [1].

[1] Max-Planck-Institut für Eisenforschung, 40237 Düsseldorf, Germany

3.10.5 Acknowledgements

Parts of this work were supported under the NSF/DFG Materials World Network program (DFG ZA 523/3-1 and NSF-DMR-1108211).

3.10.6 Keywords

Matlab ; Graphical User Interface (GUI) ; Grain Boundaries ; Polycrystalline Metals ; Grain Boundary Inclination ; Serial Polishing ; Scanning Electron Microscope (SEM).

3.11 References

3.11.1 Related Projects

Figure 3.38: MTEX

Figure 3.39: DAMASK

3.11.2 Institutions

Figure 3.40: Max-Planck-Institut fuer Eisenforschung GmbH (Duesseldorf, Germany)

Figure 3.41: Department of Chemical Engineering and Materials Science / Michigan State University (East Lansing, MI, USA)

Figure 3.42: IMDEA Materials Institute (Madrid, Spain)

Figure 3.43: Structural Integrity, Institute of Materials Engineering Australian Nuclear Science and Technology Organisation (Australia)

Figure 3.44: Physikalische Metallkunde TU Darmstadt (Darmstadt, Germany)

Figure 3.45: RWTH Aachen University (Aachen, Germany)

Figure 3.46: Solanki Research Group (Arizona State University, USA)

CHAPTER 4

References

CHAPTER 5

Contact

Authors David Mercier [1], Claudio Zambaldi [1] and Thomas R. Bieler [2].

[1] Max-Planck-Institut für Eisenforschung, 40237 Düsseldorf, Germany

[2] Chemical Engineering and Materials Science, Michigan State University, East Lansing 48824 MI, USA

CHAPTER 6

Contributors

- Raúl Sánchez Martín (IMDEA, Madrid) contributed Python code to generate *Abaqus* indentation models.

CHAPTER 7

Acknowledgements

This work was supported by the DFG/NSF Materials World Network grant references (DFG ZA 523/3-1 and NSF-DMR-1108211).

The authors are grateful to Philip Eisenlohr, Martin Crimp and Yang Su of Michigan State University, and the Max-Planck-Institut für Eisenforschung for support.

CHAPTER 8

Keywords

Matlab toolbox ; Graphical User Interface (GUI) ; Grain Boundary (GB) ; Polycrystalline Metals ; Slip Transmission ; Bi-Crystal (BX) ; Electron backscatter diffraction (EBSD) ; Instrumented indentation ; Crystal Plasticity Finite Element Method (CPFEM) ; python™ toolbox ; DAMASK.